United States
Environmental Protection
Agency

Environmental Research
Laboratory
Corvallis OR 97330

EPA-600/3-79-041
April 1979

Research and Development

Transport of Oil Under Smooth Ice

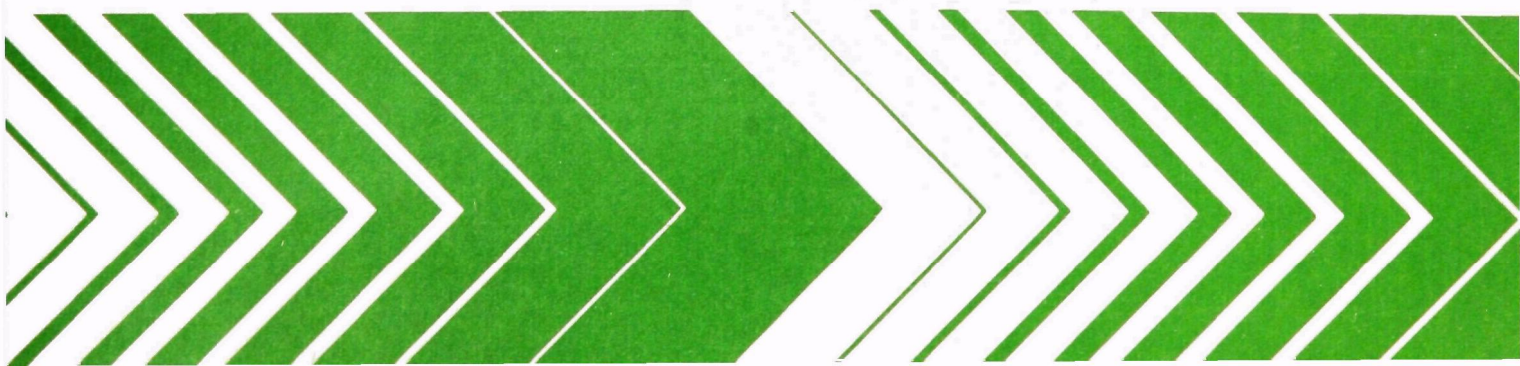

RESEARCH REPORTING SERIES

Research reports of the Office of Research and Development, U.S. Environmental Protection Agency, have been grouped into nine series. These nine broad categories were established to facilitate further development and application of environmental technology. Elimination of traditional grouping was consciously planned to foster technology transfer and a maximum interface in related fields. The nine series are:

1. Environmental Health Effects Research
2. Environmental Protection Technology
3. Ecological Research
4. Environmental Monitoring
5. Socioeconomic Environmental Studies
6. Scientific and Technical Assessment Reports (STAR)
7. Interagency Energy-Environment Research and Development
8. "Special" Reports
9. Miscellaneous Reports

This report has been assigned to the ECOLOGICAL RESEARCH series. This series describes research on the effects of pollution on humans, plant and animal species, and materials. Problems are assessed for their long- and short-term influences. Investigations include formation, transport, and pathway studies to determine the fate of pollutants and their effects. This work provides the technical basis for setting standards to minimize undesirable changes in living organisms in the aquatic, terrestrial, and atmospheric environments.

This document is available to the public through the National Technical Information Service, Springfield, Virginia 22161

EPA-600/3-79-041
April 1979

TRANSPORT OF OIL UNDER SMOOTH ICE

by

M.S. Uzuner, F.B. Weiskopf, J.C. Cox
and L.A. Schultz

ARCTEC, Incorporated
9104 Red Branch Road
Columbia, Maryland 21045

Contract No. 68-03-2232

Project Officer

Merritt A. Mitchell
Arctic Environmental Research Station
Environmental Research Laboratory
College, Alaska 99701

CORVALLIS ENVIRONMENTAL RESEARCH LABORATORY
OFFICE OF RESEARCH AND DEVELOPMENT
U. S. ENVIRONMENTAL PROTECTION AGENCY
CORVALLIS, OREGON 97330

DISCLAIMER

This report has been reviewed by the Corvallis Environmental Research Laboratory, U.S. Environmental Protection Agency, and approved for publication. Approval does not signify that the contents necessarily reflect the views and policies of the U.S. Environmental Protection Agency, nor does mention of trade names or commercial products constitute endorsement or recommendation for use.

FOREWORD

Effective regulatory and enforcement actions by the Environmental Protection Agency would be virtually impossible without sound scientific data on pollutants and their impact on environmental stability and human health. Responsibility for building this data base has been assigned to EPA's Office of Research and Development and its 15 major field installations, one of which is the Corvallis Environmental Research Laboratory (CERL).

The primary mission of the Corvallis Laboratory is research on the effects of environmental pollutants on terrestrial, freshwater and marine ecosystems; the behavior, effects and control of pollutants in lake and stream systems; and the development of predictive models on the movement of pollutants in the biosphere.

This report describes the results of a study to examine the current-driven spread of oil under a smooth ice cover. As oil and gas exploration activities increase in cold climate areas, the problems associated with oil spills become increasingly important.

James C. McCarty
Acting Director, CERL

ABSTRACT

Previous studies of oil-ice interaction have been limited to spreading under quiescent conditions. The present study examines the current driven spread of oil under a smooth ice cover. Generalized relations between current speed and oil transport rate are developed and found to be strongly dependent upon the orientation of the oil slick to the direction of current flow. Methods for application are presented.

The laboratory experiments reported were performed during October and November 1975. A draft final report was submitted to EPA for review in December 1975. This report was submitted in fulfillment of Contract 68-03-2232 under the sponsorship of the U.S. Environmental Protection Agency and work was completed in February 1979.

TABLE OF CONTENTS

	Page
INTRODUCTION	1
SUMMARY	4
CONCLUSIONS	5
BACKGROUND	7
Spread of Oil on Ice	7
Spread of Oil on Water	12
Spread of Oil Under Ice	16
ANALYTICAL APPROACH	20
EXPERIMENTAL PROGRAM	24
Test Apparatus	24
Test Procedure	26
Test Results	30
Analysis of Test Results	41
APPLICATION OF RESULTS	46
REFERENCES	48

LIST OF FIGURES

No.	Title	Page
1	Schematic Representation of Events which Could Result in Oil Spilled Beneath Ice	2
2	Relative Duration of Spreading Regimes	8
3	Reverse Flow at the Leading Edge of a Slick	15
4	Spreading of Oil Over and Under Sea Ice as Reported by Hoult	17
5	Schematic Representation of Oil Slick Transport Under Ice Cover	21
6	Schematic Depiction of ARCTEC's Ice Flume	25
7	Oil Discharge Calibration Data for Pressurized Oil Injection Chamber	27
8	Photo of Pressurized Oil Injection Chamber	28
9	Viscosity vs Temperature for Crude Oil	29
10	Photo of Oil Skimmer in Tail Tank	31
11	Photo of #2 Fuel Oil Plume Under an Ice Sheet	32
12	Photo of Cold Crude Oil Under an Ice Sheet at High Water Velocity	34
13	Schematic Representation of the Folding Phenomena at the Upstream End of a Crude Oil Slick	35
14	Slick Speed versus Current Speed for #2 Fuel Oil	39
15	Slick Speed versus Current Speed for Crude Oil	40
16	Generalized Slick Transport Relationship Based on No. 2 Fuel Oil Tests where the Slick is Oriented Parallel to the Flow	43
17	Generalized Slick Transport Relationship Based on Crude Oil Tests Where the Slick is Oriented Transverse to the Flow	44

LIST OF TABLES

No.	Title	Page
1	Equations for Oil Spreading Rate under Quiescent Conditions On or Beneath an Ice Cover	19
2	Summary of Test Data	37

LIST OF SYMBOLS

A = plan surface area (cm^2)

B, B_1, B_2 = experimentally determined coefficients

C = coefficient

C_d = drag coefficient

C_f = friction coefficient

C_s = shear force coefficient

C_w = fixed wall shear coefficient

d = water depth (cm)

F_d = form drag ($gm\text{-}cm/sec^2$)

F_f = friction force due to buoyancy ($gm\text{-}cm/sec^2$)

F_g = gravity force ($gm\text{-}cm/sec^2$)

F_i = inertia force ($gm\text{-}cm/sec^2$)

F_P = force due to a pressure drop ($gm\text{-}cm/sec^2$)

F_s = shear force at oil water interface ($gm\text{-}cm/sec^2$)

F_T = surface tension force ($gm\text{-}cm/sec^2$)

F_v = viscous force ($gm\text{-}cm/sec^2$)

g = gravitational constant = 980 cm/sec^2

h = thickness of oil slick (cm)

k, k_1, k_2 = experimental constants

ℓ = oil slick length (cm)

L = characteristic slick dimension (cm)

m = mass (gm)

N_F = densimetric Froude number $= \dfrac{U_w}{\sqrt{\Delta g h}}$

N_o = slick Reynolds number $= \dfrac{U_s\, h\, \rho_0}{\mu_0}$

N_x = characteristic Reynolds number $= \dfrac{(g\Delta L)^{1/2}}{\nu} L$

P = hydrostatic pressure ($gm/cm\text{-}sec^2$)

Q = volumetric flow rate of the oil (cc/sec)

R = radius of oil slick (cm)

t = time (sec)

T = temperature (°C)

u = velocity (cm/sec)

U = nondimensional velocity = U_s/U_w

U_s = slick velocity (cm/sec)

U_w = water velocity (cm/sec)

V = volume of oil (cc)

w = slick width (cm)

α = contact angle included in the oil

δ = water boundary layer thickness = $\sqrt{\nu t}$ (cm)

Δ = relative density difference = $\frac{\rho_w - \rho_0}{\rho_w}$

η = height of roughness element (cm)

θ = circumference of slick (cm)

κ = proportionality constant

μ_0 = viscosity of oil (gm/cm sec)

μ_w = viscosity of water (gm/cm sec)

ν = kinematic viscosity of water (cm^2/sec)

ρ_0 = density of oil (gm/cc)

ρ_w = density of water (gm/cc)

τ = shear stress (gm/cm-sec^2)

σ = net surface tension coefficient (dynes/cm)

σ_0 = surface tension coefficient (dynes/cm)

ACKNOWLEDGMENTS

The authors wish to express their appreciation to Mr. Merritt A. Mitchell of the EPA Arctic Environmental Research Laboratory for his assistance and cooperation throughout the project.

Appreciation is also extended to the ARCTEC test team for their dedication and enthusiasm under difficult conditions including low temperatures and the handling and clean-up problems inherent in laboratory testing with crude and fuel oils. The test team included engineers Francis B. Weiskopf and Peter P. Kosterich, and technicians Rick Shelsby and Roy Schnebelen, under the direction of Mehmet S. Uzuner. Jack C. Cox and Lawrence A. Schultz contributed to the final analysis of the test results.

INTRODUCTION

As more energy is consumed, it becomes increasingly more difficult to find new energy sources and to cope with the problems associated with their development. Increasing demands for energy and recent discoveries of petroleum in the arctic have resulted in the intensification of oil and gas exploration activities in the arctic. The drilling operations associated with both the exploration and development of these resources and the eventual transportation of oil to commercial centers results in an increase in the possibility of oil spills on or beneath ice.

The problem of oil spills is being investigated in order to provide information on the spreading rate of oil slicks, their transport by winds and currents, and their effects on the environment. The results of such studies will influence the selection of proper spill response techniques, both in terms of timelines and effectiveness. Most of these investigations, however, are limited to spill location prediction models, cleanup procedures, and the mobility of oil slicks in temperate waters. The behavior of oil spilled in the presence of an ice cover on quiescent waters has also been investigated to a limited extent. Little is known, however, as to how oil will behave when spilled beneath an ice cover in the presence of a current. A fundamental knowledge is required to provide a technique for predicting the movement of oil beneath an ice cover in the presence of a current, in order that the oil slick can be located, and effective spill response activities undertaken.

The following events could result in an oil spill beneath ice cover:

1. Rupture of an underwater pipeline
2. Oil well leakage or blowout
3. Natural oil seepage
4. Oil leak from a ruptured vessel.

These situations are shown schematically in Figure 1. Oil leaking from these sources will spread due to gravity forces and its internal energy while being dragged along by the flow. After the leakage is detected and stopped, the slick formed beneath the ice cover could be transported by the flow. The rate of oil transport will most likely depend upon oil properties such as viscosity and density, ice conditions such as surface roughness and porosity, and the magnitude of the water current.

The hypotheses concerning the damaging effects of oil spills to the arctic environment vary considerably from one investigator to another. Campbell and Martin [1] and Barber [2] predicted that spills in arctic regions would spread over a wide area causing large portions of the arctic ice to melt as a result of the change in the heat balance, finally affecting the climate of the entire northern hemisphere. On the other hand, Glaeser and Vance [3] and Golden [4] predicted that the spilled oil would be confined to a small area, causing limited ecological damage.

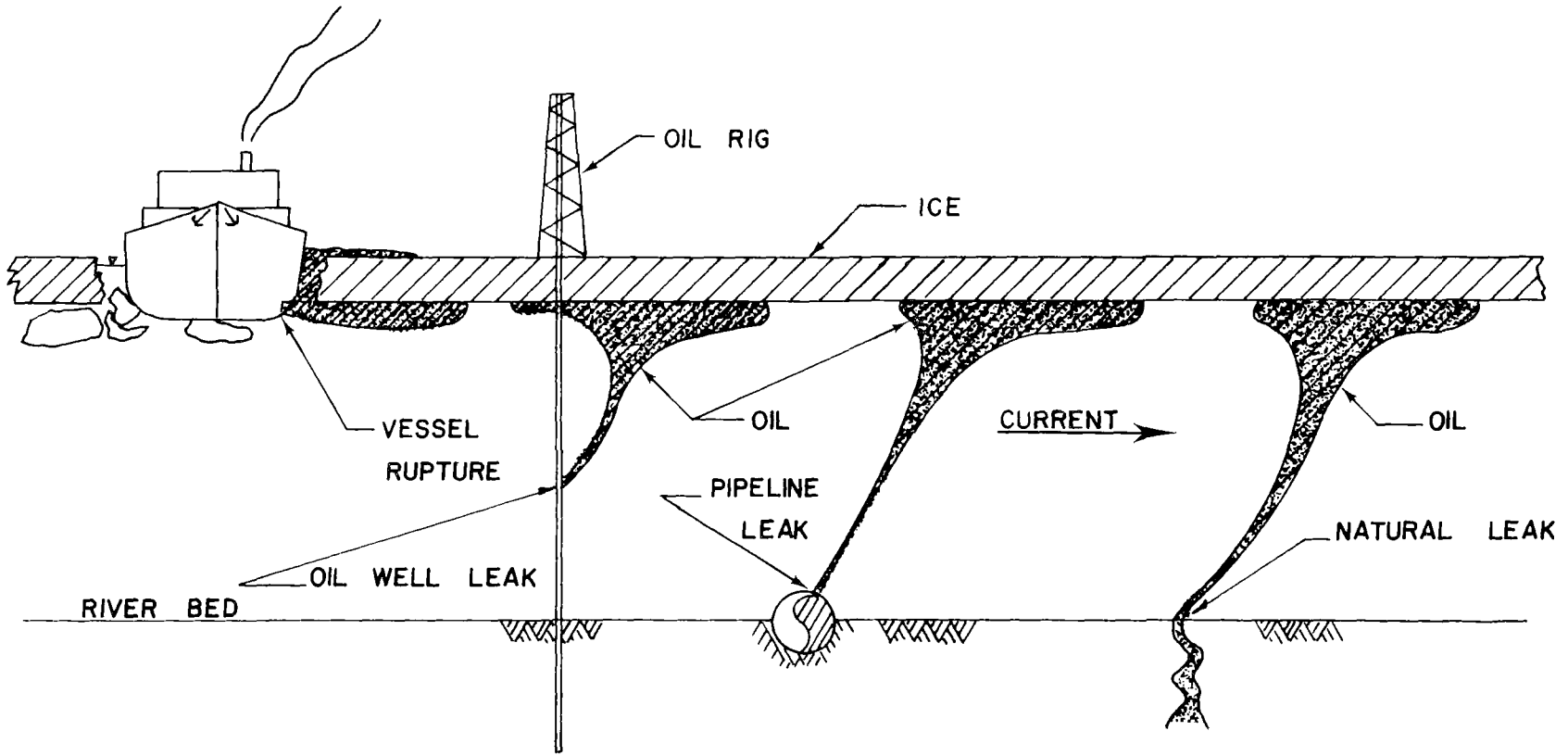

FIGURE 1. SCHEMATIC REPRESENTATION OF EVENTS WHICH COULD RESULT IN OIL SPILLED BENEATH ICE

The objective of this study is to develop a model for predicting the behavior of an oil slick in a straight stream or river of uniform depth, covered with a consolidated ice cover of uniform thickness. The water is assumed to be unidirectionally flowing at a uniform rate. It is recognized that field conditions can deviate significantly from these conditions; however, this approach allows an investigation of the physical phenomena involved.

SUMMARY

This is the final report of a test program designed to establish the transport rates for No. 2 fuel oil and crude oil under smooth ice. The oils were tested in water currents ranging from 0 to 36 cm/sec, at temperatures between -5 and 0°C.

The spill velocity of No. 2 fuel oil varied linearly with water current velocity, ranging from 0 to 11 cm/sec. The relationship between spill velocity and current velocity for crude oil follows a power curve over most of the range tested. The crude oil slick velocity ranged from 0 to 24 cm/sec.

After a thorough literature review and theoretical analysis, an analytical expression was derived in an effort to generalize the transport relation to any type of oil. The experimental results indicate that the slick movement depends on whether the slick aligns itself longitudinally or transversely to the current.

The analytical treatments developed have not been successful in defining the distinguishing characteristics for the two types of behavior, however, the proper relationship can be selected for field application after observing the orientation of the slick relative to the flow.

CONCLUSIONS

The conclusions which can be drawn from the work reported herein are as follows:

1. For an oil slick beneath a smooth uniform ice sheet, the slick velocity is related to the current velocity as follows:

Oil Type	Viscosity cp	Threshold Velocity cm/sec	Relationship of Slick Velocity, U_s, to Water Velocity, U_w cm/sec	Range of Applicability cm/sec
No. 2 Fuel	7	4	$U_s = 0.38\ U_w - 1.26$	0 - 36
Crude	24,500	8	$U_s = 8.6 \times 10^{-6}\ U_w^{4.29}$	8 - 28
			$U_s = 1.10\ U_w - 16.60$	28 - 36

2. For current velocities significantly greater than the range of applicability specified above, the tests indicate that the oil slick will become entrained in and distributed throughout the water column. The oil will then be transported in suspension with the water flow in this distributed manner, rather than along the underside of the ice surface in well-behaved slicks. Further investigation of this type of oil spill transport is beyond the scope of this study.

3. For oils other than the No. 2 fuel oil and crude oil used in the test program a theoretical analysis of the forces controlling slick transport and a comparison with the data yields a first approximation for predicting the relationship between slick velocity and water velocity for oil slicks transported beneath smooth uniform ice cover as follows:

$$(1-U)^2 = \frac{0.146}{N_F^2} + 0.450$$ for slicks oriented parallel to the flow direction.

$$(1-U)^2 = 2.15 \left(\frac{1}{N_F^2}\right)^{1.15}$$ for slicks oriented transverse to the flow direction.

4. In applying the above relationships it is necessary to know or estimate the physical properties of the spilled oil. For refined oils reasonable estimates of physical properties can be made if the actual properties are not known. For crude oils, the physical properties can vary drastically from reservoir to reservoir, and any estimate of physical properties, if the actual properties are not known, incorporates a greater level of uncertainty.

5. Significant differences were observed in the behavior of the crude oil slicks and the No. 2 fuel oil slicks. Crude oil slicks typically became shorter and wider as they moved downstream, with some thickening of the upstream portion at higher velocities. The crude oil slicks appeared to

slide along the undersurface of the ice. In contrast to this, the No. 2 fuel oil slicks typically became longer and narrower as they moved downstream and appeared to roll along the undersurface of the ice. Additional analysis beyond the scope of this study would be required to explain the reasons for these differences in behavior.

6. A single test performed using plexiglass as a simulated ice sheet revealed that the behavior of the oil slick beneath such a simulated ice cover was completely different. The crude oil used in this test adhered to the plexiglass, leaving a stationary 0.25 to 0.50 cm thick coating on the plexiglass. Neither crude oil nor No. 2 fuel oil adhered to either fresh water or salt water ice in these tests.

7. Any significant discontinuities in the ice cover, such as an open water ice edge or a slot, provided a region of containment and retention for the oil slick.

8. It should be noted that the results of these tests apply to unbounded underice oil slicks. Any contact between the slick and a boundary, such as the shores of rivers or streams, would be expected to result in the retardation of slick movement.

BACKGROUND

In order to introduce the problem of the spreading of oil and to develop a knowledge of some possible approaches to modeling oil spill behavior, previous work relating to oil spills over ice, under ice, and in open water was examined.

For the spread of an oil slick on open water, there are several analogies that can be drawn with stratified flows and saline wedges, thus the problem is fairly well formulated. However, studies of oil spreading on or under ice are very limited. The first comprehensive study of oil spreading was done by Fay [5] who defined various regimes of oil slick behavior. For systems not under any external influence, such as winds or currents, the driving forces due to hydrostatic pressure and surface tension are balanced by the retarding inertial and viscous forces.

Initially in a slick spreading on open water, the inertial forces and hydrostatic (gravity) forces dominate. As time progresses, the viscous forces become more significant than the inertial, and, finally, as the slick becomes thin enough, the surface tension force becomes more significant than the gravity force. This results in three behavioral regimes: gravity-inertial, gravity-viscous, and surface tension-viscous. In Figure 2, Fay suggests regions of applicability for each regime based on the size of the slick and the duration of spreading. As can be seen, inertial effects can be ignored fairly quickly after a spill has occurred.

Spread of Oil on Ice

Glaeser and Vance [3], McMinn [6], and Chen et al. [7], looked at the spread of oil over ice. Following the concepts outlined by Fay, they proposed a horizontal hydrostatic driving force given by

$$F_g = \int_o^h P(2\pi R)dh \ , \tag{5}$$

an inertial force given by

$$F_i = m \ \frac{du}{dt} \ , \tag{6}$$

a viscous force given by

$$F_v = \mu_0 \ \frac{du}{dh} A \ , \tag{7}$$

and a surface tension force given by

$$F_T = \sigma\theta \ . \tag{8}$$

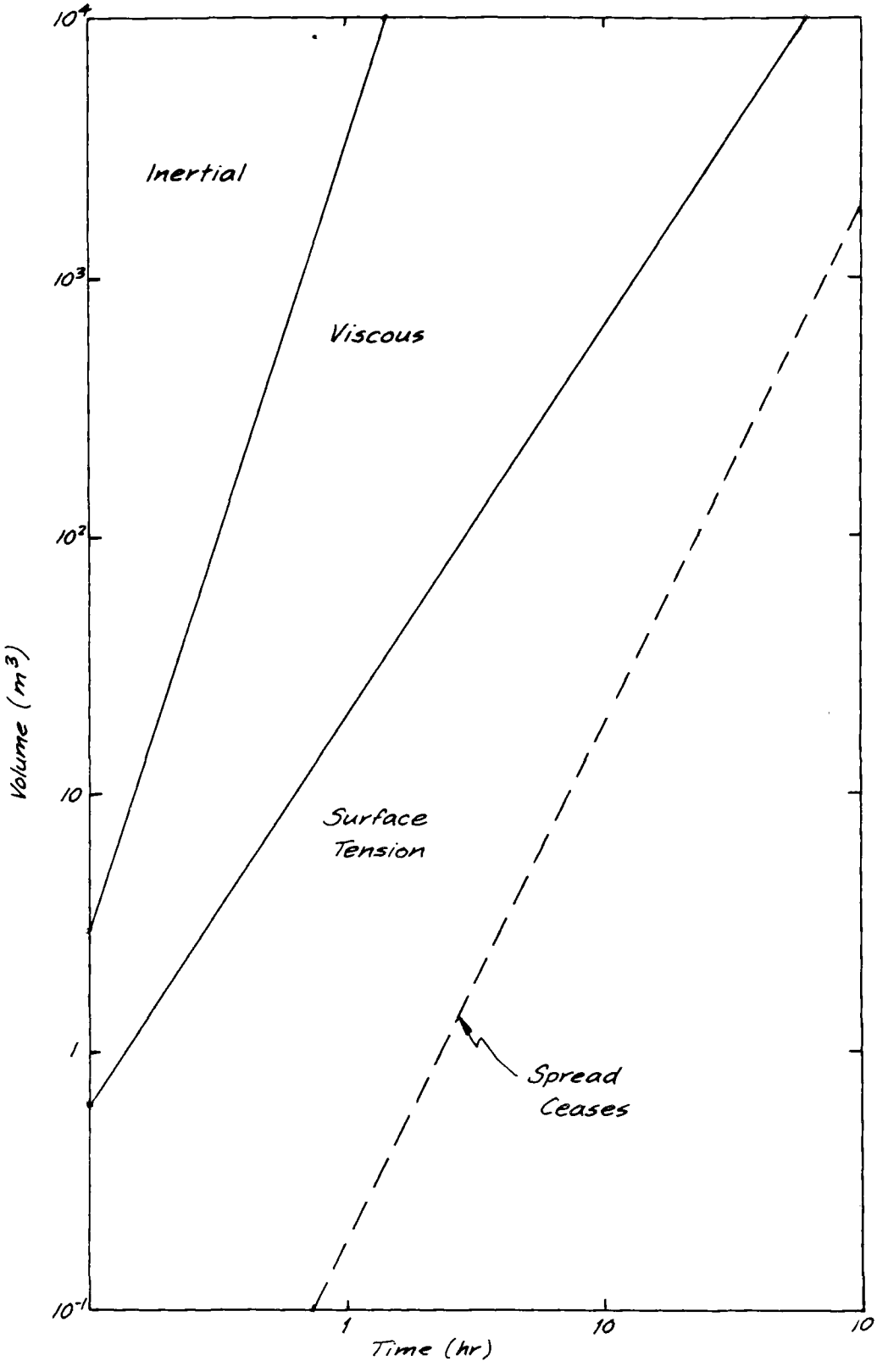

FIGURE 2. RELATIVE DURATION OF SPREADING REGIMES AFTER FAY [5].

Now if the slick is assumed to expand radially, the plan area of the slick is given as

$$\frac{V}{h} = \pi R^2 \tag{9}$$

and the circumference of the slick is

$$\theta = 2\pi R. \tag{10}$$

The hydrostatic pressure in the slick equals

$$P = \rho_0 g h \tag{11}$$

and therefore the driving force must equal

$$F_g = \int_0^h \rho_0 g h (2\pi R) dh = \rho_0 g \pi h^2 R \ . \tag{12}$$

Similarly the viscous retarding force becomes

$$F_v = \mu_0 \pi R^2 \frac{du}{dh} \ . \tag{13}$$

The surface tension becomes simply

$$F_t = 2\pi R\sigma \ . \tag{14}$$

The form of the inertia force is not so straight forward. As Hoult [8] points out, continuity must hold. Therefore if a constant flow rate is specified

$$\pi R^2 h = Qt. \tag{15}$$

The speed of advance of the front of the slick, dR/dt, can be taken as proportional to R/t.

$$dR/dt \sim R/t \tag{16}$$

Actually the slick speed is a function of both radius and change in thickness.

The inertial force then takes the form

$$F_i \sim m(R/t^2). \tag{17}$$

A balance between inertia and gravity becomes

$$m(R/t^2) \sim \rho_0 g \pi h^2 R, \tag{18}$$

but

$$m = \rho_0 \pi R^2 h, \tag{19}$$

and from Equation 15

$$h = Qt/\pi R^2. \tag{20}$$

Relation 18 then takes the form

$$\rho_0 \pi R^2 \left(\frac{Qt}{\pi R^2}\right)\left(\frac{R}{t^2}\right) \sim \rho_0 g \pi \frac{(Qt)^2}{(\pi R^2)^2} R , \tag{21}$$

or

$$R^4 \sim \left(\frac{Q}{\pi}\right) Qt^3,$$

which gives

$$R \sim \left(\frac{1}{\pi}\right)^{1/4} (gQ)^{1/4} t^{3/4} . \tag{22}$$

McMinn carried out field measurements on oil spreading over ice and observed that for his data

$$R = 1.3 \ (Q^3 g)^{0.1} t^{1/2} . \tag{23}$$

Glaeser and Vance also performed field tests and found for fixed volumes of oil

$$R = 2.75 V^{1/4} t^{3/4}. \tag{24}$$

The balance between gravity and viscous forces can be developed from Equations 12 and 13. Since oil is quite viscous, linear shear is assumed to occur in the oil as it spreads (Couette flow). This is probably a very reasonable assumption, particularly as the slick edge grows further away from the source, reducing any pressure gradient, and slowing down.

Then

$$\frac{du}{dh} = \frac{u}{h} , \tag{25}$$

and since $u \sim R/t$

$$\frac{du}{dh} = \kappa \left(\frac{R}{th}\right) , \tag{26}$$

where κ is a proportionality constant, so that

$$F_v = \mu_0 \kappa \ \pi R^2 \left(\frac{R}{th}\right) . \tag{27}$$

Then equating this to the gravity force:

$$\mu_0 \kappa \pi R^2 \frac{R}{th} = \rho_0 g \pi h^2 R, \tag{28}$$

where to be consistent with the other investigators

$$h = V/\pi R^2, \tag{29}$$

gives

$$\kappa\mu_0 \pi R^2 \frac{\pi R^2 R}{tV} = \rho_0 g \pi \left(\frac{V}{\pi R^2}\right)^2 R. \tag{30}$$

Solving for the spill radius gives

$$R^8 = \frac{\rho_0 g}{\mu_0 \pi^3 \kappa} tV^3 \tag{31}$$

or

$$R = \left(\frac{1}{\pi^3 \kappa}\right)^{1/8} \left(\frac{\rho_0 g}{\mu_0}\right)^{1/8} t^{1/8} V^{3/8} . \tag{32}$$

Instead of using the horizontal gravity driving force per unit volume

$$\frac{\rho_0 g h^2}{\ell} \frac{A}{V} \tag{33}$$

as in Equation 12, both Glaeser and Vance, and Chen, et al., chose to develop a relation for viscous spreading based on the vertical gravity force per unit volume

$$\rho_0 g h \, A/V , \tag{34}$$

which gives a different form to the expression for gravity-viscous spreading:

$$R = k_1 (\rho_0 g V^{2/3})^{1/5} (t/\mu_0)^{1/5} + k_2 V^{1/3} . \tag{35}$$

Chen, et al. experimentally solved for the constants and found $k_1 = 0.24$, and $k_2 = 0.35$.

Glaeser and Vance offer some limited data on viscous spreading which best fits a curve given in the form $R \sim t^{1/2}$.

Chen, et al. ran their experiments over varying degrees of roughness and oil temperature. They seemed to feel that their results were insensitive to changes in either of these conditions.

McMinn balanced the surface tension and the gravity force to find a critical thickness for the slick where surface tension would become important:

$$\sigma 2\pi R = \pi R \rho_0 g h^2. \tag{36}$$

Solving for h gives:

$$h = (2\sigma/\rho_0 g)^{1/2} \tag{37}$$

with

$$\sigma = \sigma_0 \ (1 - \cos\alpha). \tag{38}$$

For an oil surface tension of σ_0 = 30 dynes/cm, typical of crude oil, and an estimated contact angle on ice of α = 135°, McMinn obtains a resultant surface tension of 51 dynes/cm. Then the critical thickness becomes h_c = 0.345 cm for representative densities of oil. McMinn indicates that in field experiments of spreading oil over ice, the spreading thickness never diminished to 1/3 cm. He therefore argues that the surface tension regime does not occur for oil over ice, possibly due to the ice roughness and subsequent pocketing of the oil within the roughness matrix.

Spread of Oil on Water

The basic theory of the previous section can be extended to apply to the spread of oil on water. The horizontal gravity driving force can be easily altered to apply to a two fluid system by the inclusion of a relative density difference factor

$$\Delta = (\rho_w - \rho_0) \ / \rho_w \ . \tag{39}$$

Then the gravity equation transforms into a buoyancy equation.

$$F_g = \Delta\rho_w g\pi h^2 R. \tag{40}$$

The inertia force remains the same as before:

$$F_i \sim \ \rho_0 \pi h R^3/t^2. \tag{41}$$

The viscous force requires deeper scrutiny. As the oil slides over the surface of the water there is viscous drag exerted by the water on the oil. The viscous stress is continuous at the oil-water interface. Since the oil thickness is smaller than the water boundary layer, the velocity gradient in the oil in the vertical direction can be considered negligible compared to that in the water. There is slug flow in the oil. The retarding force due to viscous drag then becomes [8]

$$F_v \sim \mu_w \pi R^2 \ \frac{R}{t\delta} \ , \tag{42}$$

where

$$\delta = \sqrt{vt} \tag{43}$$

is the water boundary layer thickness and v is the kinematic viscosity of water

The surface tension remains as before,

$$F_T = \sigma\ (2\pi R), \tag{44}$$

where now σ is the net combination of the air-water interfacial tension, oil-water interfacial tension, and oil-air interfacial tension. Now balancing gravity and inertia forces,

$$\Delta\rho_w g\pi h^2 R \sim \rho_0 \pi\ h\ R^3/t^2, \tag{45}$$

or for a fixed volume

$$R^4 \sim \frac{\Delta\rho_w}{\pi\rho_0}\, g t^2\ V, \tag{46}$$

which gives

$$R = \left(\frac{\rho_w}{\pi\rho_0}\right)^{1/4} (\Delta g V)^{1/4} t^{1/2}. \tag{47}$$

The balance of gravity and viscous forces becomes

$$\Delta\rho_w g\pi h^2 R \sim \mu_w\ \pi\ R^2\ \frac{R}{t\delta}, \tag{48}$$

or simplifying,

$$R \sim \left(\frac{1}{\pi^2}\ \frac{g\Delta V^2\ t^{3/2}}{\nu^{1/2}}\right)^{1/6}. \tag{49}$$

Glaeser and Vance developed a similar relation for one directional flow in a channel, using

$$F_g = \Delta\rho_w g h^2 w \tag{50}$$

and

$$F_v \sim \mu_w \left(\frac{\ell}{t}\right)\ \left(\frac{1}{\sqrt{\nu t}}\right)\ (\ell w), \tag{51}$$

where

$$V = \ell w h. \tag{52}$$

Balancing these gives

$$\ell \sim \left(\frac{\Delta g V^2}{w^2\sqrt{\nu}}\right)^{1/4}\ t^{3/8}. \tag{53}$$

Field data for surface tension spreading is probably the hardest to acquire, however, a relation can still be developed by balancing the surface tension force with the viscous force

$$2\pi R\sigma \sim \mu_w \pi \frac{R^3}{t\delta}, \tag{54}$$

or

$$R^2 \sim \frac{2}{\mu_w} \sigma\sqrt{\nu}\ t^{3/2}, \tag{55}$$

and simplifying gives

$$R \sim \sqrt{2}(\sigma^2 t^3/\rho_w^2 \nu)^{1/4}. \tag{56}$$

Hoult [8] looked at detailed properties of the slick motion and developed similarity solutions to the governing equations of motion. In the inertia regime he found the spill radius to be described as:

$$R_{max} = \phi_{max} (g\Delta)^{1/(3+n)} L^{(2+n)} / (3+n)_t \ 2/(3+n), \tag{57}$$

where for one directional flow $n = 0$, and $L = V^{1/2}$,

and for axisymmetric flow $n = 1$, and $L = V^{1/3}$.

For one directional spreading ϕ_{max} was theoretically calculated to be 1.57. The experimental value was found to be 1.5. For axisymmetric flow ϕ_{max} was calculated to be 1.14.

In the viscous regime the similarity solution takes the form

$$\frac{R_{max}}{L} = \phi_{max} \left[\frac{g\Delta}{L} t\right]^{(3-n)/16} N_x^{1/(8+4n)}, \tag{58}$$

where N_x is a characteristic Reynolds number:

$$N_x = \frac{(g\Delta L)^{1/2}}{\nu} L. \tag{59}$$

Because the boundary conditions are not uniquely defined for this case, ϕ_{max} was determined from experimental results:

$$\phi_{max} = 1.5 \quad \text{for } n = 0$$

$$\phi_{max} = 1.12 \quad \text{for } n = 1.$$

It also appears that, based on this analysis, a regime exists downstream from the leading edge of the slick where reverse flow occurs. This feature is shown in Figure 3.

For the surface tension regime the similarity solution is the same for both the one directional and axisymmetrical cases:

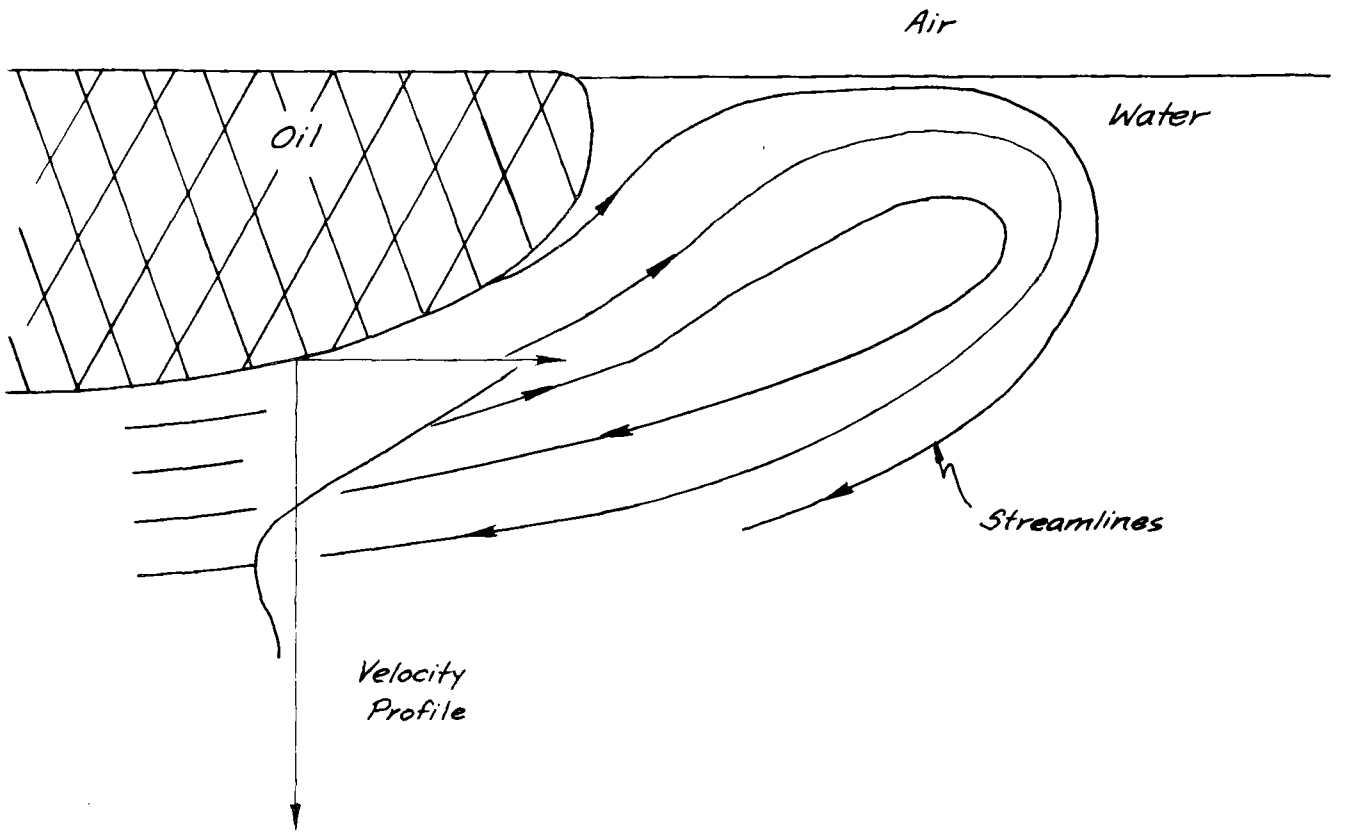

FIGURE 3. REVERSE FLOW AT THE LEADING EDGE OF SLICK.

$$R_{max} = \phi_{max} \left(\frac{\sigma^2 t^3}{\rho_w \nu} \right)^{1/4} \tag{60}$$

In this case the theoretical values become

$$\phi_{max} = 0.665 \quad \text{for } n = 0,$$

$$\phi_{max} = 0.128 \quad \text{for } n = 1.$$

The experimental value of ϕ_{max} for $n = 0$ was found to be 1.33. No reason for this variation was given.

Spread of Oil Under Ice

Hoult [9] approached the problem of oil spread both under and over ice by arguing that the only important retarding force was due to energy dissipation as the slick moved across a rough surface. This would be proportional to a pressure drop or head loss in the fluid. The retarding force would also have to be proportional to the frontal area of roughness seen by the approaching oil. This force can then be given as

$$F_P = k \ 2\pi R \eta \ \rho_0 \left(\frac{dR}{dt} \right)^2 \tag{61}$$

where $\frac{dR}{dt}$ is given as in Equation 16 and η is the equivalent roughness height.

The driving gravity force is identical with that given in Equation 40 as

$$F_g = \Delta \rho_w g \pi h^2 R.$$

Equating these two forces gives

$$R = \left(\frac{1}{2\pi^2 k} \right)^{1/6} \left(\frac{\rho_w}{\rho_0} \right)^{1/6} \left(\frac{\Delta g Q^2}{\eta} \right)^{1/6} t^{2/3} \tag{62}$$

Experimental data for this case is plotted in Figure 4. Hoult suggests that the value of $\left(\frac{1}{2\pi^2 k} \right)^{1/6}$ should be 0.25 based upon the data; however, a value of 0.55 seems to be more satisfactory. The expression

$$R = 0.55 \left(\frac{\Delta \rho_w g Q^2}{\rho_0 \eta} \right)^{1/6} t^{2/3} \tag{63}$$

is also plotted in Figure 4. For comparison, Equation 32 for viscous spreading can be adjusted for oil under ice by again introducing the relative density difference factor or Δ (Equation 39), giving

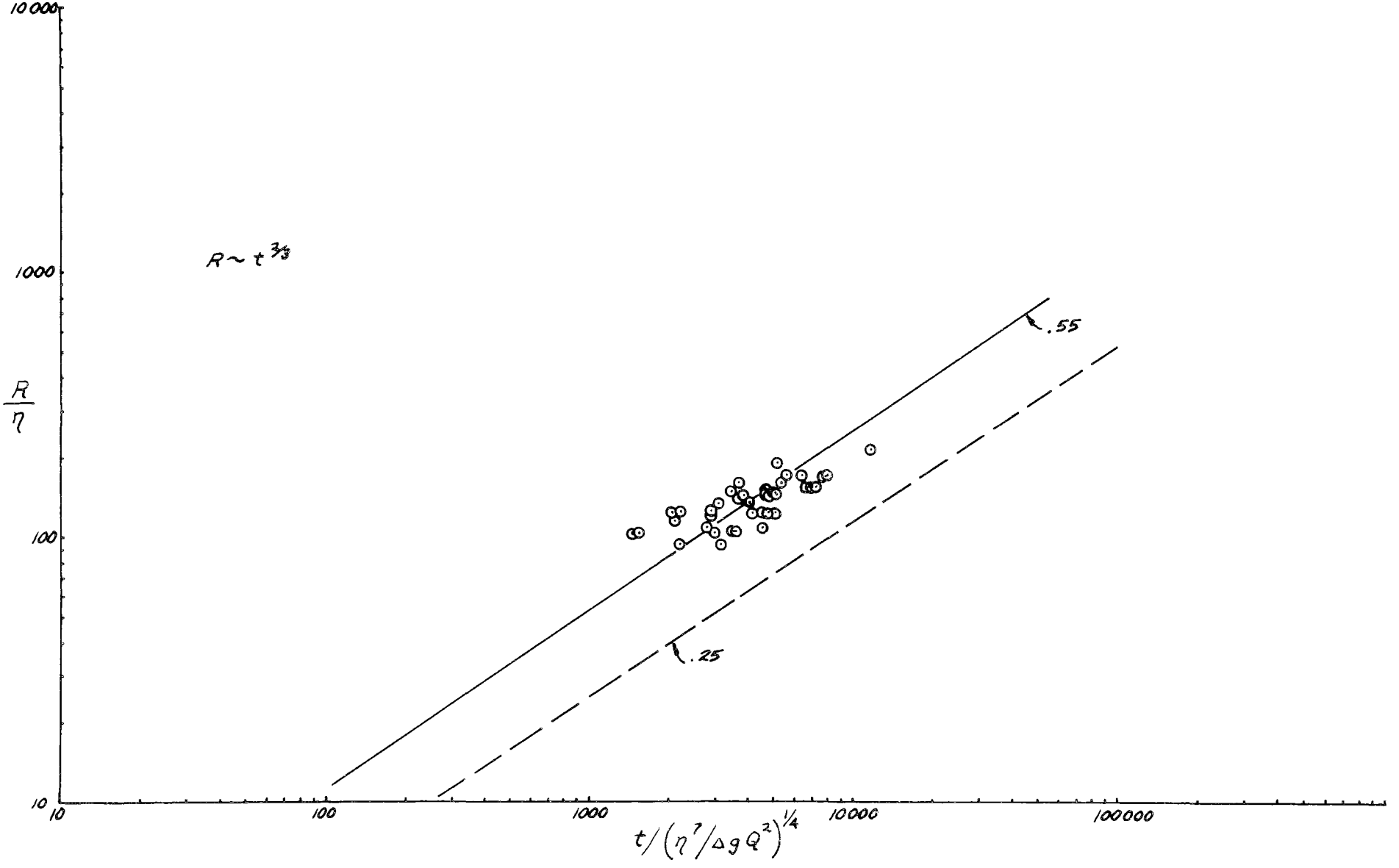

FIGURE 4. SPREADING OF OIL OVER AND UNDER SEA ICE AS REPORTED BY HOULT [9]

$$R = \left(\frac{1}{\pi^3} \right)^{1/8} \left(\frac{\Delta \rho_w g}{\mu_0} \right)^{1/8} V^{3/8} t^{1/8} \tag{64}$$

By inserting some typical values for Δ, ρ_w, g, μ_0, and η into both equations 36 and 65, it becomes apparent that these two relations differ significantly only with respect to time over a broad range of values for the flow rate.

A prediction for the equilibrium thickness of a slick based upon the balance of surface tension and hydrostatic forces can also be made by introducing Δ into Equation 38:

$$h = \left(\frac{2\sigma}{\Delta \rho_w g} \right)^{1/2} . \tag{65}$$

Again $\sigma = \sigma_0 (1 \quad \cos\alpha)$, where α is the angle included in the oil, and σ_0 is now the interfacial surface tension. MacKay et al. [10] indicate that typical underice oil slick thicknesses will range from 0.9 to 1.2 cm.

The various theories for oil spreading are listed in Table 1. All of the relations can only be approximate since the speed of advance of the slick front is only known in a proportional sense. An exact relation for slick radius as a function of time must follow a similarity solution, as carried out by Hoult [9], which assumes that velocity is proportional to R/t.

In general, long term spreading of oil on water will probably be controlled by surface tension so that

$$R \sim \sqrt{2} (\sigma^2 t^3 / \rho_w^2 \nu)^{1/4} . \tag{66}$$

For oil spreading on or under ice the viscous regime will dominate so that

$$R \sim \left(\frac{1}{\pi^3} \right)^{1/8} \left(\frac{\Delta \rho_w g}{\mu_0} \right)^{1/8} V^{3/8} t^{1/8} . \tag{67}$$

If the ice is rough, the oil will spread according to

$$R = 0.55 \left(\frac{\Delta \rho_w g Q^2}{\rho_0 \eta} \right)^{1/6} t^{2/3} . \tag{68}$$

TABLE 1. SUMMARY OF THEORETICAL OIL SPREADING UNDER QUIESCENT CONDITIONS

REGIME	OIL ON WATER	OIL ON ICE	OIL UNDER ICE	INVESTIGATION
Gravity-Inertia		$R \sim \left(\frac{1}{\pi}\right)^{1/4} (gQ)^{1/4} t^{3/4}$ (radial spreading)		McMinn Glaeser & Vance
	$R \sim \left(\frac{\rho_w}{\pi\rho_o}\right)^{1/4} (\Delta g V)^{1/4} t^{1/2}$ (radial spreading)			Hoult 72 Fay
Gravity-Viscous		$R \sim \left(\frac{1}{\pi^3}\right)^{1/8} \left(\frac{\rho_w g}{\mu_o}\right)^{1/8} t^{1/8} V^{3/8}$ (radial spreading)		Chen et al. (Corrected) Glaeser & Vance
	$R \sim \left(\frac{1}{\pi^2} g \frac{\Delta V^2}{\nu^{1/2}} t^{3/2}\right)^{1/6}$ (radial flow)			Hoult 72 Fay
	$R \sim \left(\frac{\Delta g V^2}{\omega^2 \sqrt{\nu}}\right)^{1/4} t^{3/8}$ (one directional)			Glaeser & Vance
			$R \sim \left(\frac{1}{\pi^3}\right)^{1/8} \left(\frac{\Delta\rho_w g}{\mu_o}\right)^{1/8} t^{1/8} V^{3/8}$ (radial spreading)	Chen et al. (Adjusted)
Surface Tension-Viscous	$R \sim \sqrt{2}(\sigma^2 t^3/\rho_w^2 \nu)^{1/4}$ (radial spreading)			Hoult 72 Fay
Head Losses			$R = 0.55 \left(\frac{\Delta\rho_w g Q^2}{\rho_o \pi}\right)^{1/6} t^{2/3}$	Hoult 74 (Corrected)

ANALYTICAL APPROACH

When oil is released into a stream beneath an ice cover, the slick will take several different forms depending upon the flow conditions, oil properties and roughness of the ice cover. A theory universally applicable to oil slicks in general, describing the behavior of different types of oil on or beneath various types of ice covers, would be unyielding and impractical. The following analysis is therefore only applicable within the framework of the cases considered in this study. The goal of the analysis is to derive the most comprehensive analytical relation for the motion of crude oil and No. 2 fuel oil beneath a smooth ice cover. In the analytic model, a complete force balance equation for an element of rectangular planform taken from an oil slick beneath uniform ice cover and subject to a current would include a liquid-solid shear drag at the ice-oil interface, a liquid-liquid shear drag at the oil-water interface, a negative surface tension spreading coefficient at the oil-ice-water interface, and gravity forces. Preliminary tests indicated that the gravity forces and surface tension forces could be eliminated from the model since they either cancelled each other or were overpowered by the other forces. The modified analysis presented, which is of a more simplified nature, examines the force balance in the streamwise direction for the patch of oil. As such, it considers only the frictional force at the ice-oil interface, the shear force at the oil-water interface, and a form drag due to the shape of the slick. The oil injected under the ice cover is assumed to be at the same temperature as the ice, so that the ice does not melt as a result of heat flux from the oil to the ice and thereby affect oil movement. Moreover, the analysis is valid only after the oil forms a slick beneath the ice cover. The analysis does not account for the transient conditions associated with the injection of the oil, the behavior of the oil plume as it surfaces to the bottom of the ice, and the initial spreading of the oil at the ice surface. The analysis is concerned only with the subsequent transport of the oil slick beneath the ice due to the water current.

Consider that a known amount of oil is injected into the stream beneath a continuous ice sheet as depicted schematically in Figure 5. After the oil is released, it will rise to the bottom of the ice cover as a result of buoyancy forces, and it will either collect in an inverted mound, as was the case with crude oil or will form a uniform layer, as was the case with No. 2 fuel oil. Depending upon the type and orientation of the slick, different forces govern the force balance on the slick. The driving forces acting on the slick are the form drag, which results from the pressure difference between the upstream and downstream ends of the slick, and the shear force at the oil-water interface, which is due to the water current. The retarding force is the sliding or rolling friction between the ice surface and the oil, treating the oil as a solid.

The slick geometry in this analysis can be represented by a mean height,

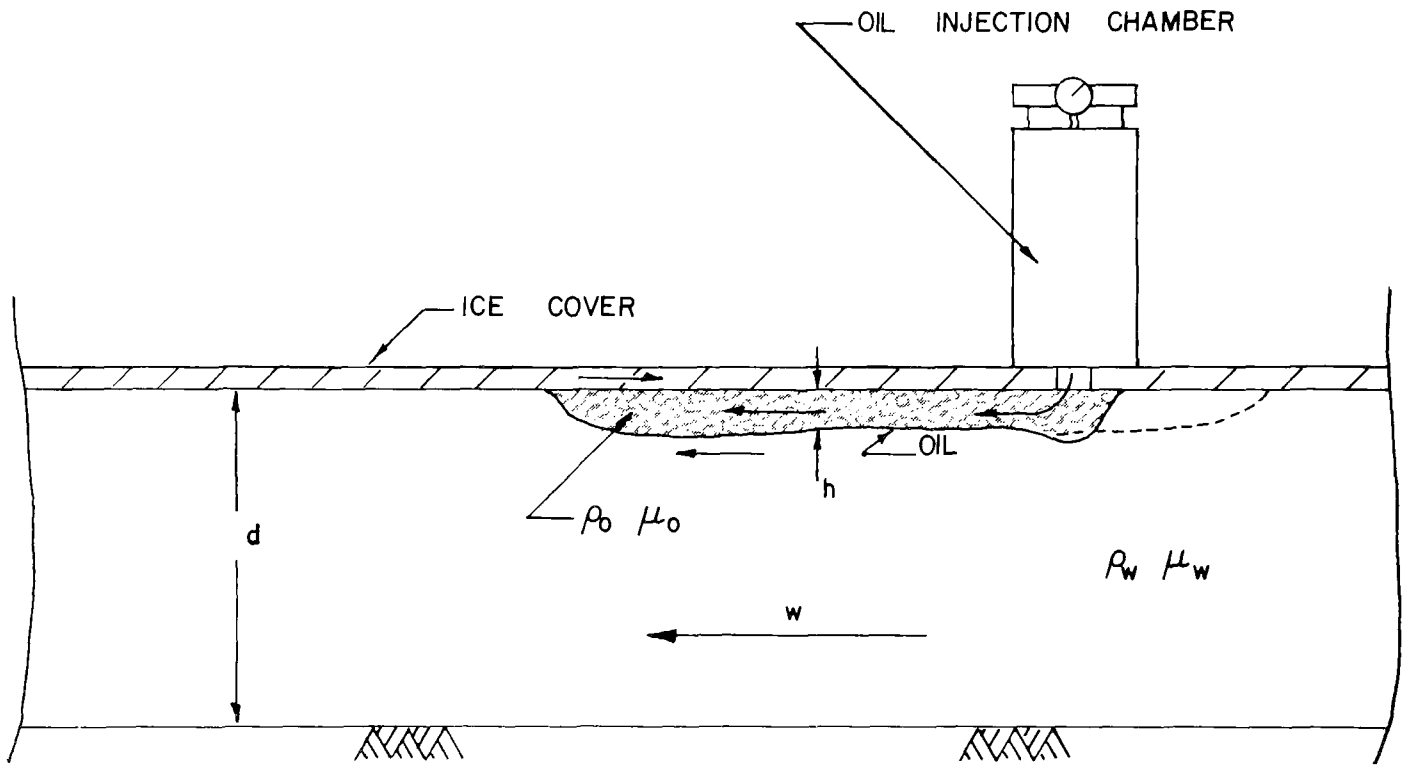

FIGURE 5. SCHEMATIC REPRESENTATION OF OIL SLICK TRANSPORT UNDER AN ICE COVER

h, width, w, and length ℓ. The volume of the oil slick, V, is then:

$$V = h\ \ell\ w\ . \tag{69}$$

Form Drag: The drag is caused by the difference in pressure exerted on the upstream and downstream ends of the slick, and is expressed as:

$$F_d = \frac{1}{2}\ C_d\ \rho_w\ (U_w - U_s)^2\ w\ h \tag{70}$$

where C_d is a drag coefficient, ρ_w is the water density, U_w is the mean water velocity, and U_s is the mean slick velocity. Note that this force becomes more important as the slick formed beneath the ice cover thickens.

Shear Force at Oil-Water Interface: This is a driving force due to the shear applied to the oil at the oil-water interface by the moving current. Assume an averaged shear stress based upon the relative velocity between the two fluids:

$$F_s = \frac{1}{2}\ C_s\ \rho_w\ (U_w - U_s)^2\ w\ \ell \tag{71}$$

The shear stress coefficient, C_s is not the same as a drag coefficient over a flat plate. Jeffreys [11] defined this coefficient as a sheltering coefficient, usually applied to cases of wind and waves. By considering the pressure normal to a wavy surface he estimates C_s to be 0.3. Jirka et al [12], looking at flow near the interface of two fluids give a relation for C_s as $C_s = 0.64\ C_w$, where $C_w = 16/N_O$, N_O being the oil Reynolds number. The range of C_s for a moving slick using this approach would typically be 0.01 to 0.1. The most significant point is that values of C_s for this case are at least one to two orders of magnitude larger than those for a rigid flat plate.

Ice-Oil Interfacial Friction Force: The retarding force on the slick as it slides downstream as a "rigid" body can be estimated from the normal buoyant force that the slick exerts on the ice cover and a kinetic friction factor.

$$F_f = C_f\ (\rho_w - \rho_0)\ gV \tag{72}$$

The coefficient C_f is a solid-solid type of friction factor.

Force Balance: For equilibrium, the retarding forces must balance the driving forces.

$$F_f = F_d + F_s \tag{73}$$

By substituting the expressions for F_f, F_d, and F_s from Equations 70, 71, and 72, the expression for the force balance becomes:

$$C_f (\rho_w - \rho_0) ghw\ell = \frac{1}{2} C_d \rho_w (U_w - U_s)^2 wh + \frac{1}{2} C_s \rho_w (U_w - U_s)^2 w\ell \quad (74)$$

This can be nondimensionalized through the introduction of the densimetric Froude number:

$$N_F = \frac{U_w}{\sqrt{\Delta g h}} \quad (75)$$

The general form for the force balance then becomes:

$$(1 - U)^2 = \left[\frac{2C_f}{C_d \frac{h}{\ell} + C_s} \right] \frac{1}{N_F^2} \quad . \quad (76)$$

Provided that the coefficients can be estimated, the spread of any slick could be expected to follow a relation of the form:

$$(1 - U)^2 = \frac{B}{N_F^2} \quad . \quad (77)$$

The presence of the term h/ℓ in Equation 76 should be noted. The affect of this term is to make form drag important if the shape of a slick becomes narrow in the direction of the current, i.e., orients itself transverse to the flow. If the slick becomes very long, shear stress becomes the more important driving force.

EXPERIMENTAL PROGRAM

The analytical model of oil slick movement beneath smooth ice cover contains coefficients which must be determined experimentally. To quantify these coefficients and verify the theory, experiments were conducted in ARCTEC's Ice Flume. The apparatus and the test procedure used in these tests are described below.

Test Apparatus

The facility and the main apparatus used in the tests consist of the flume and the pressurized oil injection chamber. The instruments used in determining the oil properties are described in the Test Procedures section.

Flume. The experiments for this investigation were conducted in ARCTEC's insulated, glass walled Ice Flume which is depicted schematically in Figure 6. The test section of the flume is 13.7 m long, 0.94 m wide, and 0.61 m deep. The flume is located in ARCTEC's insulated low temperature test facility. Ice is made in the flow section by a patented cryogenic system. The glass walls, channel bottom, return pipe, and the drive unit are insulated to prevent ice formation inside the system during the freezing process. Insulation panels for the glass walls are removable in sections along the flume where under-ice observations are made. There are two glass windows, 6 m apart, along the channel floor for under-ice photography.

Flume capacity is about 170 liters per second with 15 cms of water achieved by a ten horsepower variable speed motor and a 25 cm diameter axial flow pump. The maximum allowable water depth is 46 cms with 18 cms of freeboard. The discharge of the flume is measured by a conventional precalibrated orifice-meter mounted between two flanges of the return line. The piezometers of the orifice-meter are connected to a differential manometer located near the flume inside a specially built, heated container.

Pressurized Oil Injection Chamber. The pressurized oil injection chamber (hereinafter referred to as a box) was designed to inject oil at a point just below the bottom surface of the ice sheet thru a 2.0 cm hole drilled in the middle of the box. The volume of the box is 26.5 liters. This unit is turned on or off by pneumatically raising or lowering a two way piston that has a plug mounted on the end of it. A system of three way valves which controls the piston is manipulated so that one side of the two way piston is being bled to atmosphere while the other side is being pressurized. After the plug has been lifted from the hole, the pressure inside the box is increased by adjusting a throttle valve to a point such that the oil plume is penetrating about 2 to 4 cms into the flow. The volume of oil in the box is monitored with a surface-following float attached to a lever arm and connected to a 10 turn potentiometer. By reading the resistance change of the

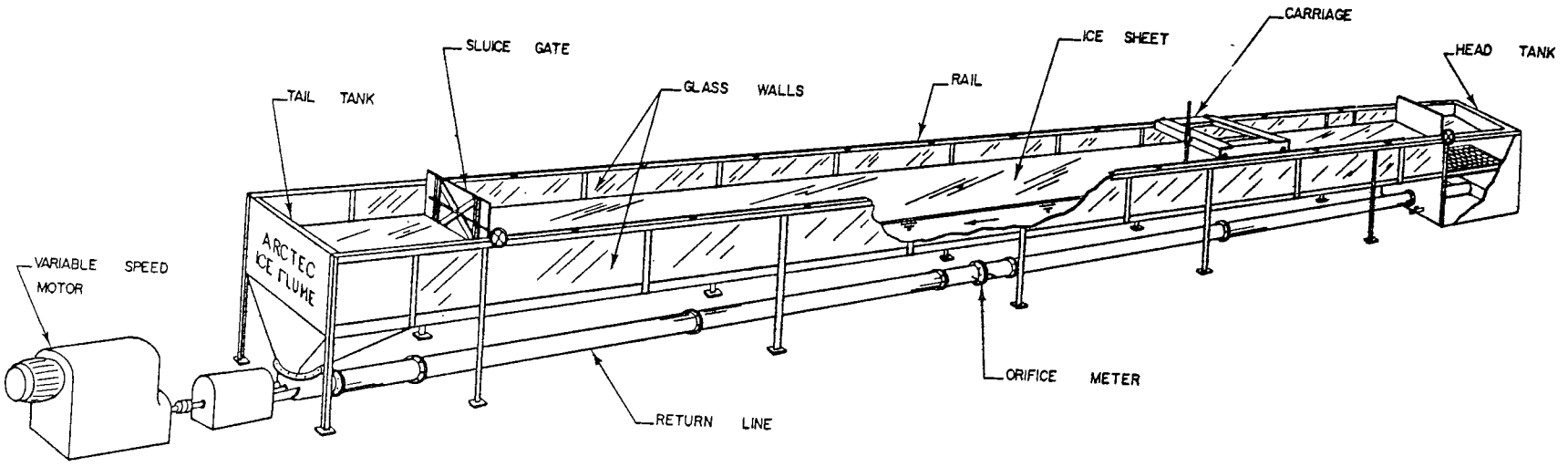

FIGURE 6 SCHEMATIC DEPICTION OF ARCTEC'S ICE FLUME

potentiometer on a 5 place digital multimeter, the volume of oil remaining in the chamber can be established. The oil is turned off after a predetermined volume of oil has been injected into the flow. The calibration data for the box is presented in Figure 7 and a photograph of the box is shown on Figure 8.

Test Procedure

The first step for each test was to freeze an ice sheet in the flume using ARCTEC's cryogenic freezing system. The freezing procedure can be remotely controlled from the control room. While the ice sheet was being frozen, the properties of the oil to be used in the tests were determined. This was done before each test to monitor any property variations due to temperature changes or nonuniformity of oil samples. The properties measured were viscosity, surface tension, and specific gravity. All measurements were made inside the small cold room located near the refrigerated test facility using instruments and procedures meeting ASTM specifications.

The instruments used to measure the specific gravity were ASTM approved hydrometers meeting specification E 100-66. The appropriate hydrometer was lowered into the sample and allowed to settle. After equilibrium temperature is reached, the hydrometer scale and the temperature of the sample were recorded.

A Brookfield Viscometer, Model LVT, was used to measure apparent viscosity. The viscometer operates by rotating a cylinder or disc in the fluid and measuring the torque necessary to overcome the viscous resistance to the induced movement. This is accomplished by driving the immersed element, which is called a spindle, through a beryllium copper spring. The degree to which the spring is wound, indicated by the position of a red pointer on the viscometer's dial, is proportional to the viscosity of the fluid for any given speed and spindle. The viscometer is able to measure over a number of ranges, since for a given drag or spring deflection, the actual viscosity is proportional to the spindle speed, and is also related to the spindle's size and shape. For a material of given viscosity, the drag will be greater as the spindle size and/or rotational speed increase. The minimum range of any viscometer model is obtained by using the largest spindle at the highest speed, the maximum range by using the smallest spindle at the slowest speed. These procedures are in accordance with ASTM specification D 2983-72. The results obtained for crude oil are shown in Figure 9.

A Fisher Surface Tensiometer Model 20 was calibrated and used to measure the oil/water surface tension. The Model 20 is a torsion-type balance instrument, the kind currently specified by ASTM in Methods D-971 and D-1331. In this instrument, a platinum-irridium ring of precisely known dimensions is suspended from a counter-balanced lever arm. The arm is held horizontal by torsion applied to a taut stainless steel wire, to which it is clamped. Increasing the torsion in the wire raises the arm and the ring,

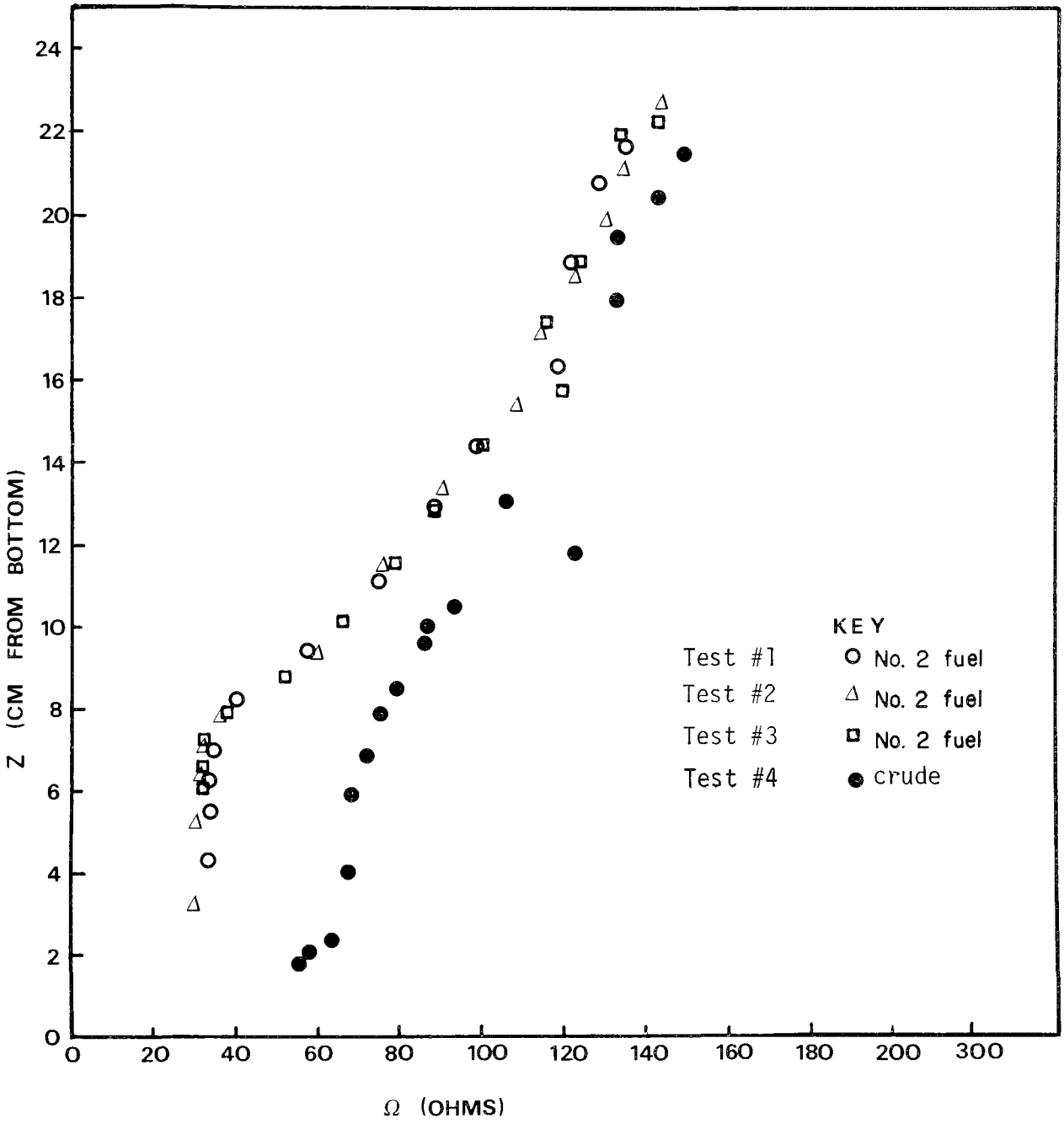

FIGURE 7 OIL DISCHARGE CALIBRATION DATA FOR PRESSURIZED OIL INJECTION CHAMBER

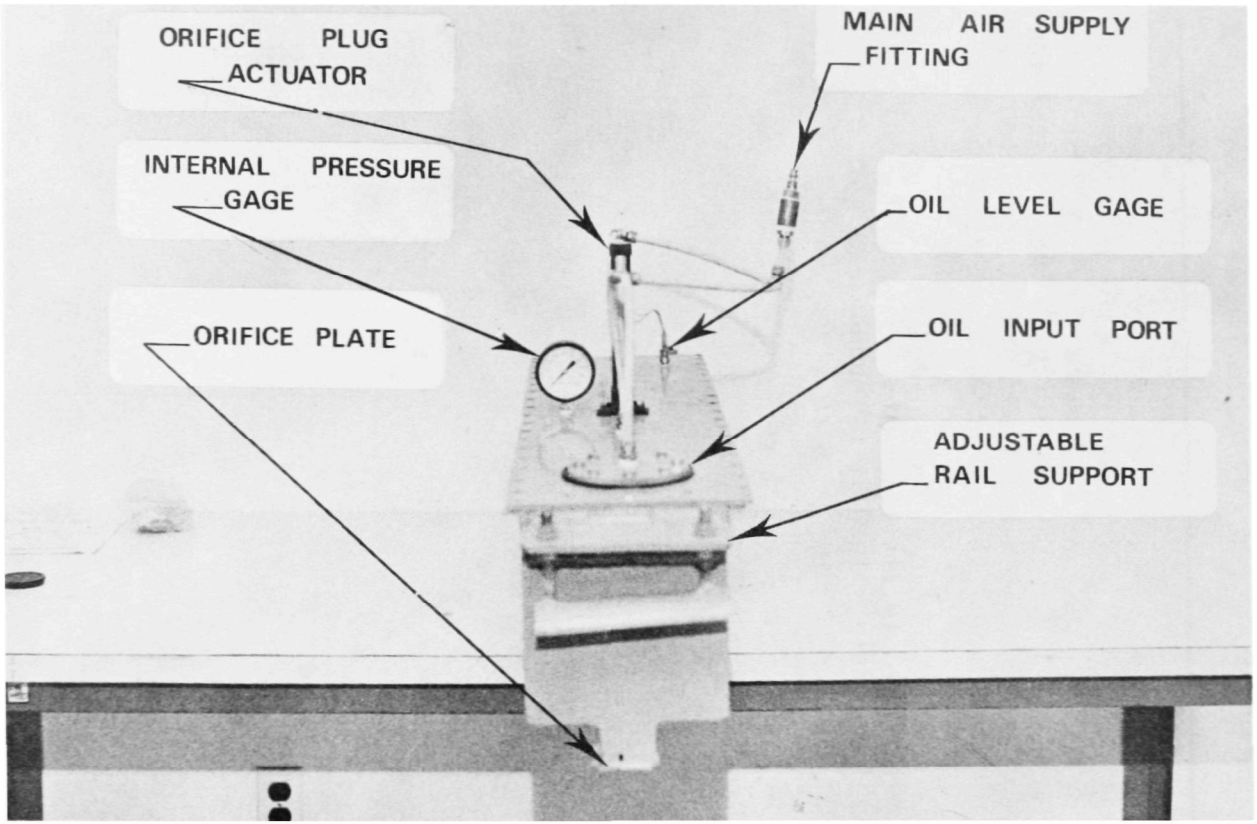

FIGURE 8 PHOTO OF PRESSURIZED OIL INJECTION CHAMBER

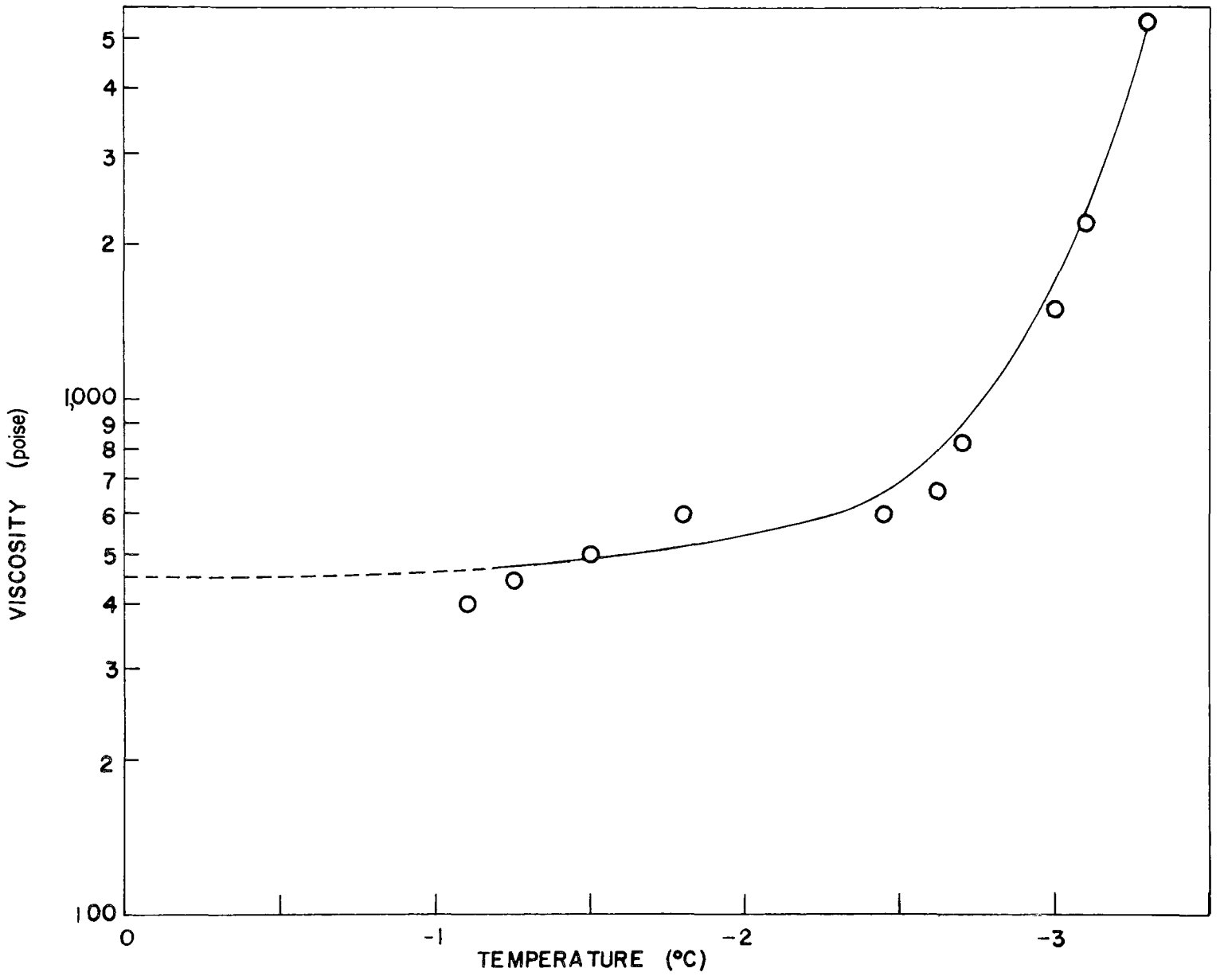

FIGURE 9. VISCOSITY vs. TEMPERATURE FOR CRUDE OIL

which carries with it a film of the liquid in which it is immersed. The force necessary to pull the test ring free from this surface film is measured. The surface tensiometer shows this "apparent" surface tension on a calibrated dial. The dial readings are then converted to "true" values by using the correction factors provided with the instrument.

Initally, the oil/water surface tension was measured in the cold room using oil at about 0°C. At this temperature the crude oil was too viscous to establish a sharp interface with the water; thus the surface tension tests could not be conducted in a reasonable amount of time (note that ASTM standards put a time limitation on the existence of the oil/water interface before the test is conducted, i.e., after the oil/water interface is formed the test must be conducted within a certain time period). However, it is generally correct that interfacial surface tension is a strong function of the materials involved, and weak function of the temperatures of the materials.

Thermometers used in this program were accurate to 0.1°C. Temperatures were recorded when measuring viscosity, surface tension and specific gravity in both the pre- and post-test series.

After the ice sheet was frozen, the flume was prepared for the test and the test apparatus was installed. The flume was then turned on to the desired flow rate and oil was injected using the pressurized oil injection chamber. As the oil entered the flow and started to move downstream, the position of the oil slick was recorded as a function of time, and still photographs and movies of the oil slick motion were taken. After the oil was turned off, the length of the slick was measured (when appropriate) as the slick traveled down the flume. When the downstream edge of the slick reached the tail tank, the test was terminated. At this point the flume was turned off and cleanup procedures were started. The cleanup consisted of mounting an oil skimmer, as shown in Figure 10, in the tail tank and pumping off the top layer of the oil/water system. This was then pumped through an oily water separator, or directly into waste oil containers. Absorbent rags and cloths were used to clean up the remaining oil.

Test Results

After an ice sheet of desired thickness was frozen and the apparatus was installed in the flume, each experiment was started by turning on the flume to a predetermined flow rate. The discharge was adjusted by varying the speed of the drive motor and by checking the differential manometer attached to the piezometers of the orifice-meter located along the return line of the flume. After a steady state condition was achieved, approximately 18.9 liters of oil was injected into the stream through a 2 cm diameter hole on the bottom of the pressurized oil injection chamber. The oil was forced through the hole at a slight pressure so that the flow rate was approximately 0.12 liters/sec. After leaving the box, the plume formed by the oil was bent because of the flow, and rose to the underside of the ice sheet due to buoyancy as shown in Figure 11. Depending upon the jet Reynolds Number, the oil plume either broke up into large drops as in the case of No. 2 fuel oil, or formed a continuous plume

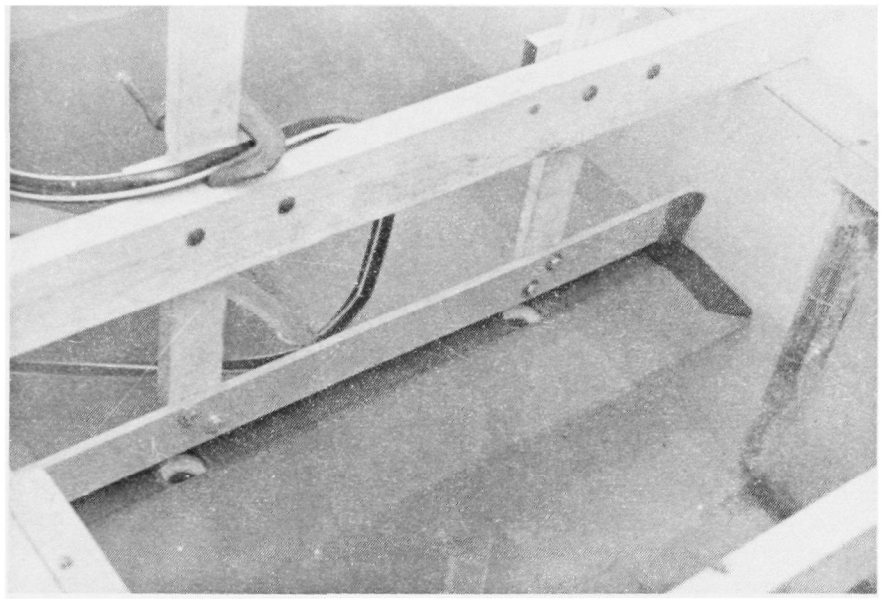

FIGURE 10 PHOTO OF THE OIL SKIMMER IN THE TAIL TANK

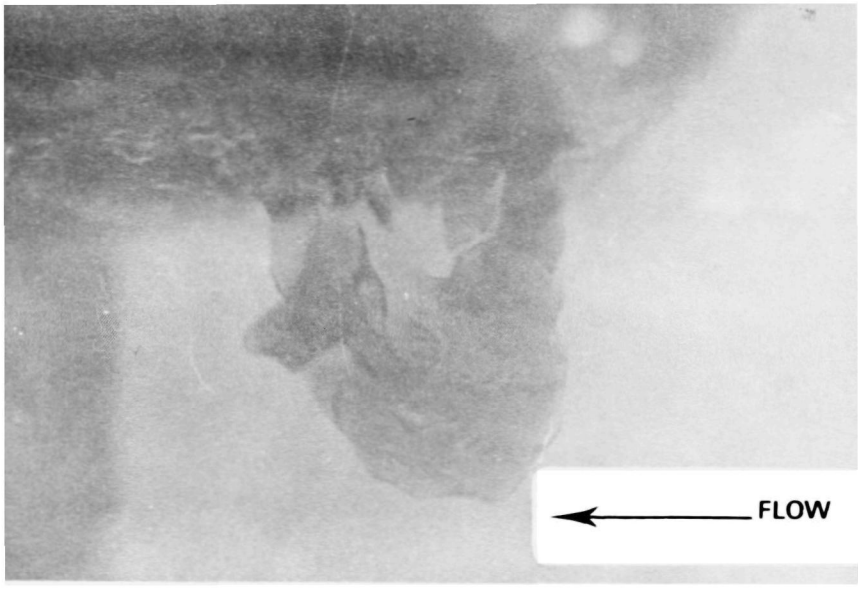

FIGURE 11 PHOTO OF NO. 2 FUEL OIL PLUME UNDERNEATH AN ICE SHEET

before rising to the underside of the ice sheet as in the case of the crude oil.

Another difference between the No. 2 fuel oil and the crude oil was that the gravity forces acting on the No. 2 fuel oil were larger than for the crude oil because of its lower density. The difference in vertical forces resulted in different trajectories for the plume which consequently caused the two plumes to come into contact with the ice sheet at different locations along the flume.

As portions of the slick left the box region, the crude oil and No. 2 fuel oil exhibited distinct behavior patterns. Typically, the slick formed by the crude oil was short and wide, oriented transversely to the flow, and moved downstream like a solid body. At low water velocities the crude oil rose to the underside of the ice cover in the region of the pressurized oil injection chamber, and spread both laterally and streamwise. In this case, the slick remained attached to the box for a long time before being swept downstream with the flow. The slick deformed very slightly, and there were no oil/water interfacial waves. At high water velocities, the plume moved further downstream before it came into contact with the ice sheet. Because of the high viscosity, the crude oil did not spread transversely; instead, it initially kept its rope-like shape as it was carried downstream by the flow as shown in Figure 12. Subsequently, the rope broke and formed small elongated patches of oil. The oil slicks compacted into a mass whose transverse dimensions were greater than their streamwise dimensions. As the slick formed and moved downstream, its upstream edge thickened as a result of the water accelerating around the edge of the slick as shown in Figure 13. Some patches of crude, torn from the sides of the major slick would move downstream at a higher velocity than the main, but again would orient transverse to the flow.

The appearance of a fuel oil slick was considerably different than that of the crude oil slick. The slick formed by the fuel oil had a uniform thickness of about 0.5 cm and a very smooth oil/water interface, the only roughness being the interfacial waves observed at the higher velocities. It was observed that the fuel oil slick "rolled" along the underside of the ice sheet. At high water velocities, small patches of oil would separate from the main slick as it traveled down the flume. Some of the patches would recombine with the main slick, whereas others would move downstream independently. These small patches would travel at a higher speed than the parent.

After the first few tests had been run with No. 2 fuel oil it was noted that the oil slick thickness quickly reached a limiting value, determined by a balance between the negative surface tension spreading coefficient and the buoyant forces. This same limiting thickness condition also seemed to be apparent in the static water cases that were run with the cold crude oil. In these cases the oil slick was allowed to sit overnight after it had been confirmed that the slick had a constant thickness. Also, for one flume test where the crude oil was significantly warmer than 0°C, the spread rate was very

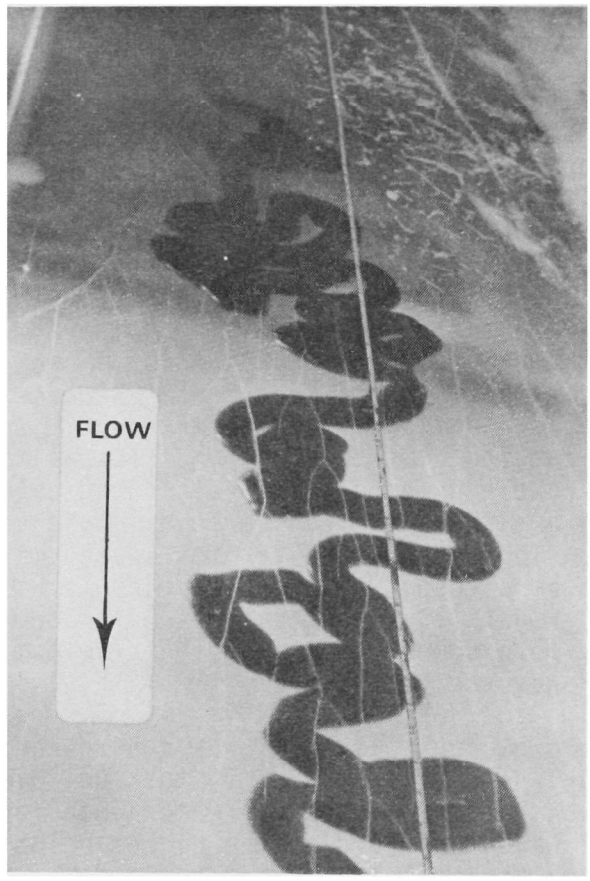

FIGURE 12 PHOTO OF COLD CRUDE OIL UNDER AN ICE SHEET AT HIGH WATER VELOCITY

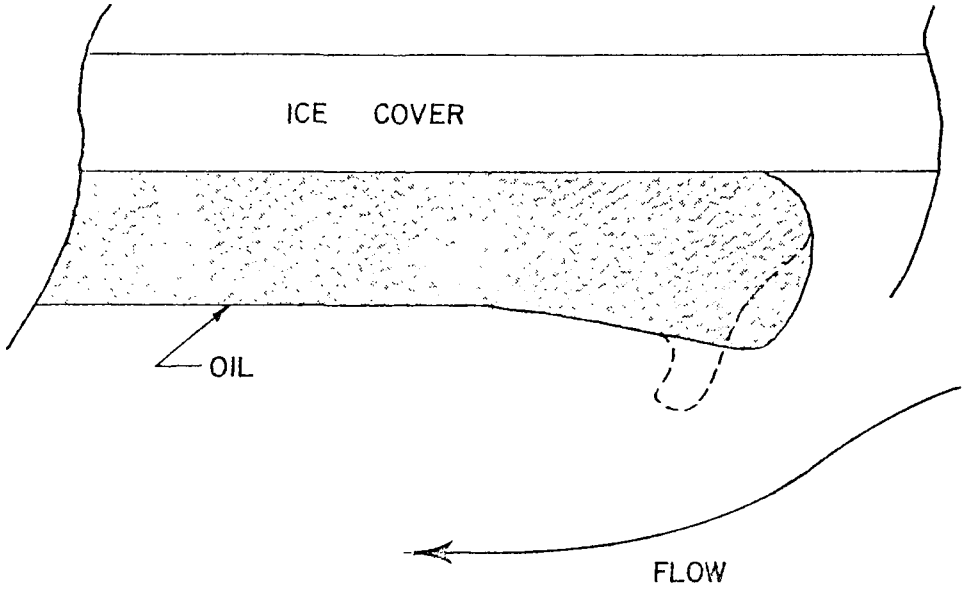

FIGURE 13. SCHEMATIC REPRESENTATION OF THE FOLDING PHENOMENA AT THE UPSTREAM END OF A CRUDE OIL SLICK

rapid and the crude seemed to reach a limiting thickness. However, for the cases where the crude oil was very cold, i.e., below 0°C, the oil collected where the plume came into contact with the bottom of the ice sheet for low water velocities, or was swept away as soon as it arrived at the bottom of the ice sheet for the high water velocities. For those cases where the slick did not move, it was noted that during the course of the experiment the slick did not become appreciably thinner. Because the oil is so viscous, it cannot flow on a time period comparable to that of the No. 2 fuel oil, or within a time period comparable to the length of the experiment.

Tests conducted with salt water did not show any significant differences in the behavior of the oil. However, it was observed that oil droplets entrained in the water later became enmeshed in the pores of the ice upon rising to the ice/water interface. This "trapped oil" gave the underside of the ice sheet a dirty appearance. It can be concluded from this that additional clean-up after melting may be necessary for oil spills beneath salt water ice covers if emulsification occurs at the time of the spill.

In order to investigate the feasibility of using plexiglass as a simulated ice cover, a test was conducted with plexiglass in the same manner as the other tests. A plexiglass sheet, 0.83 cm thick and 180.0 cm long, was placed in the flume approximately 300 cm downstream from where the oil was injected. The ice was cut out and removed, and the plexiglass fitted into its place. The plexiglass sheet was placed in the flume approximately 45 minutes before the initiation of the test in order to allow it to come to thermal equilibrium. As the oil passed under the simulated cover, the slick was slowed down and was finally stopped. After the oil slick had stopped moving, the test was allowed to continue for approximately 15 minutes before the pumps were turned off in order to be certain that the slick had completely stopped. When the sheet was lifted from the surface of the water at the completion of the test, a uniform coating of oil remained adhered to the sheet. The oil beneath a plexiglass sheet therefore showed a totally different behavior than oil under an actual ice cover.

A test to simulate the dynamics of a hot oil slick beneath an ice cover was also performed. In this test, approximately 11 liters of hot crude oil at 50°C was injected into the stream from a simulated point source located approximately 5 cms below the ice/water interface.

Qualitatively, the hot crude oil behaved in a manner analogous to the low viscosity No. 2 fuel oil. The high water velocity broke up the jet, and the large patches were carried downstream before they rose to the surface at an open water region; consequently, no interaction between the hot oil and the ice was observed.

The physical parameters measured during each test in order to quantify and verify the analytical model are listed in Table 2. Figure 14 and 15 are plots of the mean slick velocity versus current velocity for No. 2 fuel oil and crude oil. Data points from tests 20 and 21 have been deleted from these plots.

TABLE 2. SUMMARY OF TEST DATA

Test No.	Water Velocity, U_w (cm/s)	Oil Type	Slick Velocity*, U_s (cm/s)	Oil Viscosity, μ_0 (centipoise)	Slick Thickness, h (cm)	Oil Density, ρ_0 (gm/cm^3)	Water Depth, d (cm)	Oil Temperature,+ T_0 (°C)	Interfacial Surface Tension, σ (dyn/cm)	Froude Number, N_F	Nondimensional Velocity, U
1	5.0	#2Fuel	0.4	7	0.5	0.86	27.8	-	-	0.60	0.08
2	14.0	#2Fuel	3.5	7	0.5	0.86	27.4	1.5	-	1.69	0.25
3	5.4	#2Fuel	0.6	7	0.5	0.86	25.6	-2.6	16.6	0.65	0.11
4	9.9	#2Fuel	2.0	7	0.5	0.86	23.5	1.0	12.8	1.20	0.21
5	15.1	#2Fuel	4.1	8	0.5	0.86	23.6	-1.4	14.8	1.82	0.27
6	20.1	#2Fuel	6.6	7	0.5	0.86	22.7	-0.4	19.3	2.43	0.33
7	20.1	Crude	2.3	25000	1.3	0.91	23.0	-0.8	69.0	1.88	0.12
8	9.8	Crude	0.0	15000	1.3	0.91	21.7	-0.8	38.0	0.92	0.00
9	20.0	Crude	3.7	15000	1.3	0.91	21.7	-0.8	38.0	1.87	0.18
10	20.0	Crude	4.4	15000	1.3	0.91	21.7	-	38.0	1.39	0.22
11	14.9	Crude	0.5	25500	1.3	0.91	23.4	1.8	15.8	1.33	0.03
12	14.3	Crude	0.5	25500	1.3	0.91	23.4	1.8	15.8	1.84	0.04
13	19.7	Crude	3.4	36500	1.3	0.91	16.1	-0.3	17.0	2.26	0.17
14	24.2	Crude	10.6	36500	1.3	0.91	16.1	-	17.0	1.48	0.44
15	15.8	Crude	1.9	36500	1.3	0.91	16.1	-	17.0	2.19	0.12
16	24.8	Crude	12.3	25500	1.3	0.90	13.4	2.0	15.8	2.67	0.50
17	30.1	Crude	15.7	25500	1.3	0.90	13.4	2.9	15.8	2.67	0.52
18	36.1	Crude	24.6	25500	1.3	0.91	13.4	5.5	15.8	3.37	0.68
19	19.4	Crude	4.4	25500	1.3	0.91	13.4	1.5	15.8	1.81	0.23

TABLE 2. SUMMARY OF TEST DATA (CONTINUED)

Test No.	Water Velocity, U_w (cm/s)	Oil Type	Slick Velocity*, U_s (cm/s)	Oil Viscosity, μ_0 (centipoise)	Slick Thickness, h (cm)	Oil Density, ρ_0 (gm/cm³)	Water Depth, d (cm)	Oil Temperature,+ T_0 (°C)	Interfacial Surface Tension, σ (dyn/cm)	Froude Number, N_F	Nondimensional Velocity, U
20	21.3	#2Fuel	9.8	7	0.5	0.86	10.5	2.4	13.4	2.57	0.46
21	24.5	#2Fuel	16.7	7	0.5	0.86	10.5	2.2	13.4	2.95	0.68
22	19.5	#2Fuel	5.8	7	0.5	0.86	13.9	-0.1	10.1	2.35	0.30
23	27.2	#2Fuel	9.7	7	0.5	0.86	13.9	0.0	10.1	3.28	0.36
24	32.3	#2Fuel	10.7	7	0.5	0.86	13.9	0.0	10.1	3.90	0.33
25	25.0	#2Fuel	7.8	7	0.5	0.86	13.9	0.1	10.1	3.02	0.31
26	9.1	#2Fuel	2.4	7	0.5	0.86	14.9	-0.4	9.3	1.10	0.27
27	14.9	#2Fuel	4.7	7	0.5	0.86	14.9	-1.0	9.3	1.80	0.32
28	21.0	#2Fuel	7.0	7	0.5	0.86	14.9	-1.0	9.3	2.54	0.33
29	14.5	Crude	1.0	25500	1.3	0.91	15.2	-1.5	16.4	1.35	0.07
30	19.4	Crude	4.8	25500	1.3	0.91	15.2	0.7	16.4	1.81	0.25
31	25.8	Crude	10.6	25500	1.3	0.91	15.2	-2.3	16.4	2.41	0.41

* Computed as the change in downstream position of the slick edge divided by the change in time and average overall readings.

+ Temperature of oil prior to being injected into the stream.

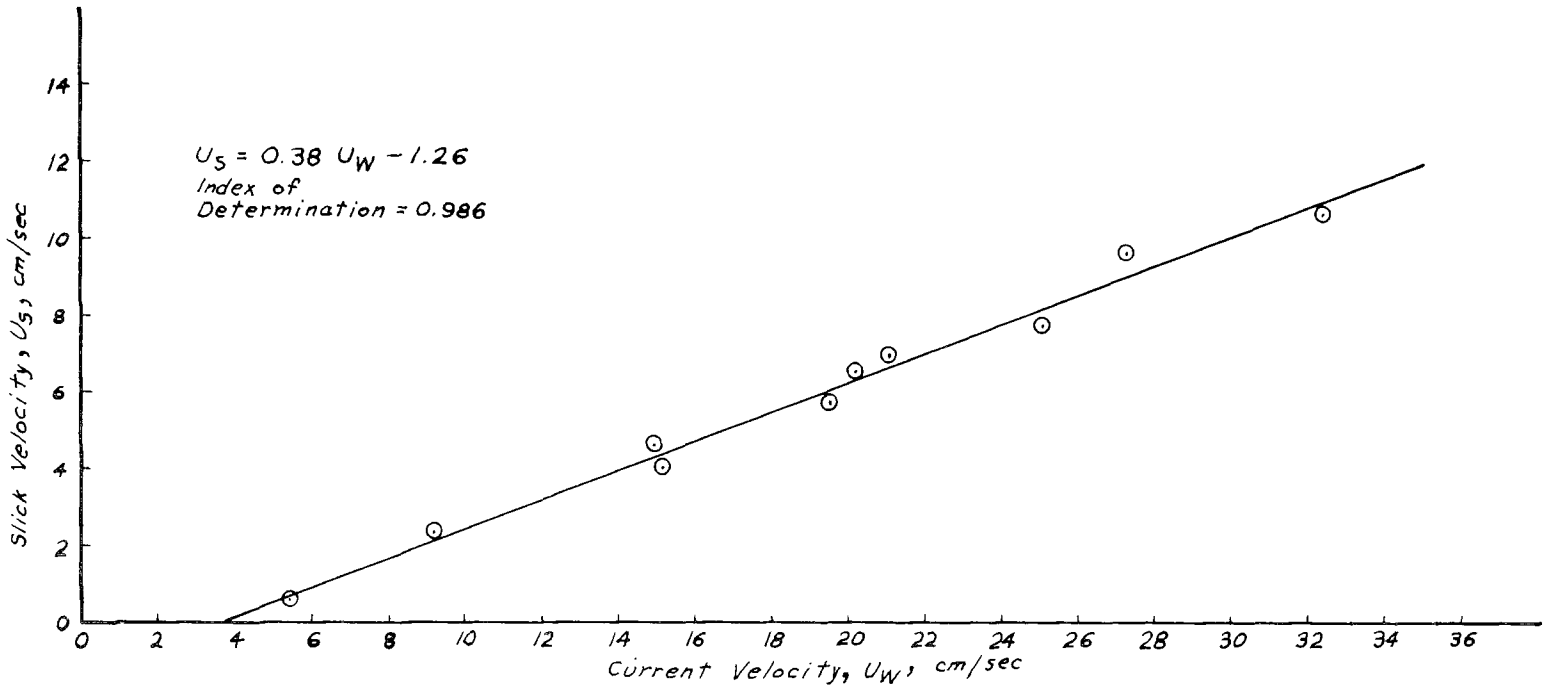

FIGURE 14. PLOT OF SLICK VELOCITY vs. CURRENT VELOCITY FOR No. 2 FUEL OIL

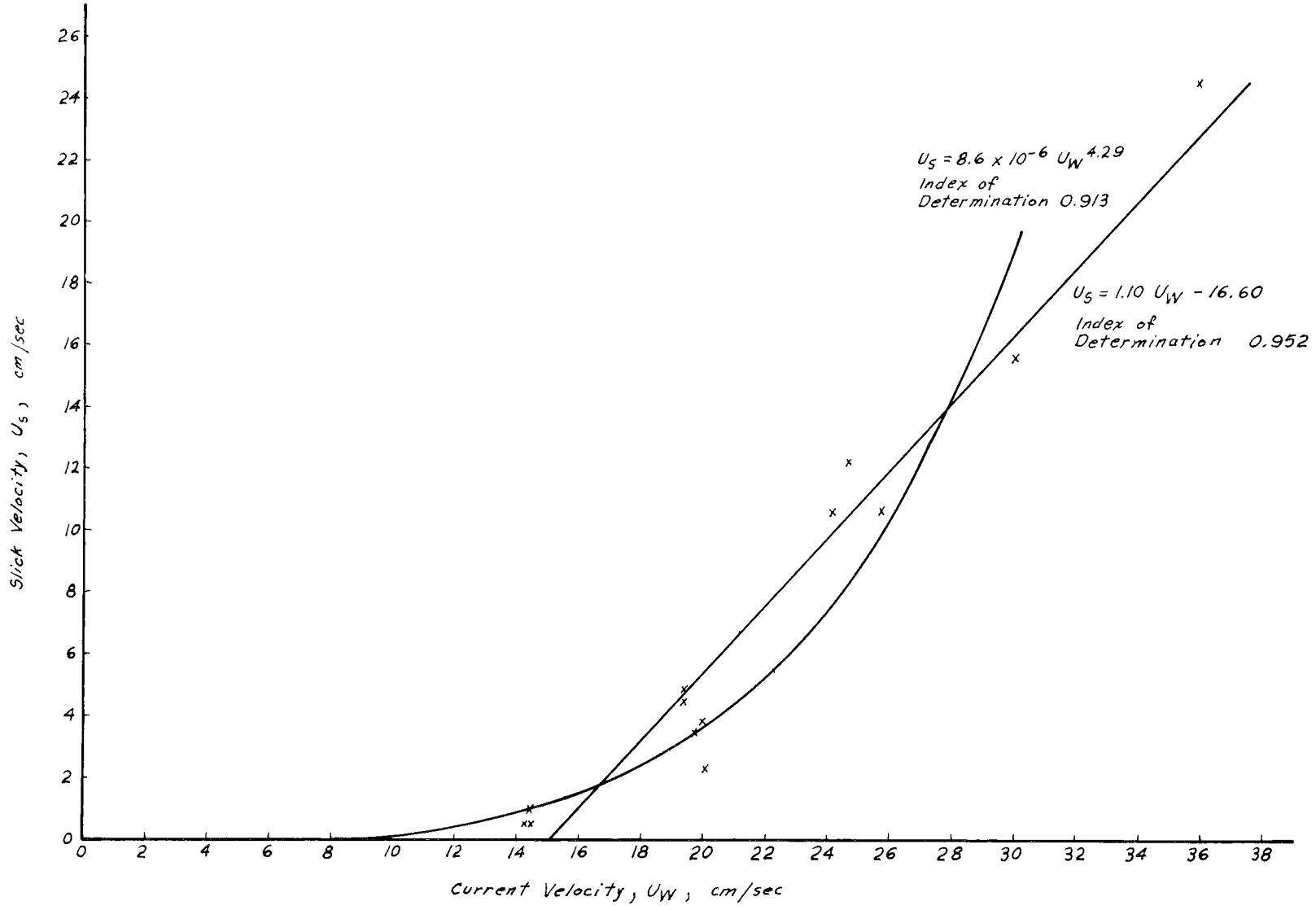

FIGURE 15. PLOT OF SLICK VELOCITY vs. CURRENT VELOCITY FOR CRUDE OIL.

Movies of tests 20 and 21 show the No. 2 fuel oil slick to be highly broken up. The test results are therefore suspect, particularly in view of the fact that smaller slicks seem to move at much higher velocities than larger slicks for the same current speed.

The No. 2 fuel oil slick speed exhibits a very strong linear relation with the current speed. The threshold velocity for smooth ice is seen to be approximately 4 cm/sec. The slick velocity follows the relation:

$$U_s = 0.38\ U_w - 1.26, \text{ for } 0 \leq U_w \leq 36. \tag{78}$$

The slick speed for crude oil also appears to follow a linear relationship for high current speeds; however, this best fit line is seen to predict a threshold velocity which the data shows to be too high. A power curve has therefore also been fit through the data. The result is a more reasonable threshold velocity with the slope of the curve approximately that of a straight line for intermediate velocities. By this method the threshold velocity is estimated to be 8 cm/sec, and the crude oil slick velocity relation becomes:

$$U_s = 8.6 \times 10^{-6}\ U_w^{4.29}, \quad \text{for } 8 \leq U_w \leq 28. \tag{79}$$

This curve should really not be extended above a current speed of 28 cm/sec, however. As seen in Figure 15, above this value the linear expression is judged to be more representative:

$$U_s = 1.10\ U_w - 16.60, \text{ for } 28 \leq U_w \leq 36. \tag{80}$$

Analysis of Test Results

In order to generalize the test results for oils of any type, it is necessary to test the theoretical equation derived earlier. Recall that the force balance equates the friction force to the sum of the forces due to form drag and interfacial shear:

$$F_f = F_d + F_s\ . \tag{73}$$

From observations of the shape of the crude oil slicks and the No. 2 fuel oil slicks, it is apparent that a different force dominates in each case. The No. 2 oil slick always remained long and narrow. The dominant driving force here is the shear applied to the interface. The force balance could then be approximated by:

$$F_f = F_s\ . \tag{81}$$

Conversely, crude oil slicks always oriented themselves to the flow, becoming very short in length measured with the flow direction. Form drag must therefore dominate for crude slicks, and the force balance can be approximated by:

$$F_f = F_d \, . \tag{82}$$

For the No. 2 fuel oil, Equation 76 reduces to:

$$(1 - U)^2 = \frac{B_1}{N_F^2} \quad , \tag{83}$$

where

$$B_1 = \frac{2C_f}{C_s} \, . \tag{84}$$

This form of relation is plotted with the data in Figure 16. The constants are then determined from a best fit of the data as:

$$(1 - U)^2 = \frac{0.146}{N_F^2} + 0.450 \, . \tag{85}$$

The presence of the constant term may at first appear unsettling, however there could be momentum losses due to wave formation at the oil water interface. This loss would be solely a function of the current speed, and would be of the form $\rho_w U_w^2$. The force balance would then become of the form:

$$F_f = F_s + C \rho_w U_w^2 \tag{86}$$

For large enough Froude numbers, this wave motion would tend to dominate, eventually causing breakup of the slick.

For crude oil Equation 76 reduces to:

$$(1 - U)^2 = \frac{B_1}{N_F^2} \tag{87}$$

where

$$B_2 = \frac{2C_f \ell}{C_d h} \, . \tag{88}$$

This form of relation is plotted with the data in Figure 17. The constants are then determined from a best fit of the data as:

$$(1 - U)^2 = 2.15 \left(\frac{1}{N_F^2}\right)^{1.15} \tag{89}$$

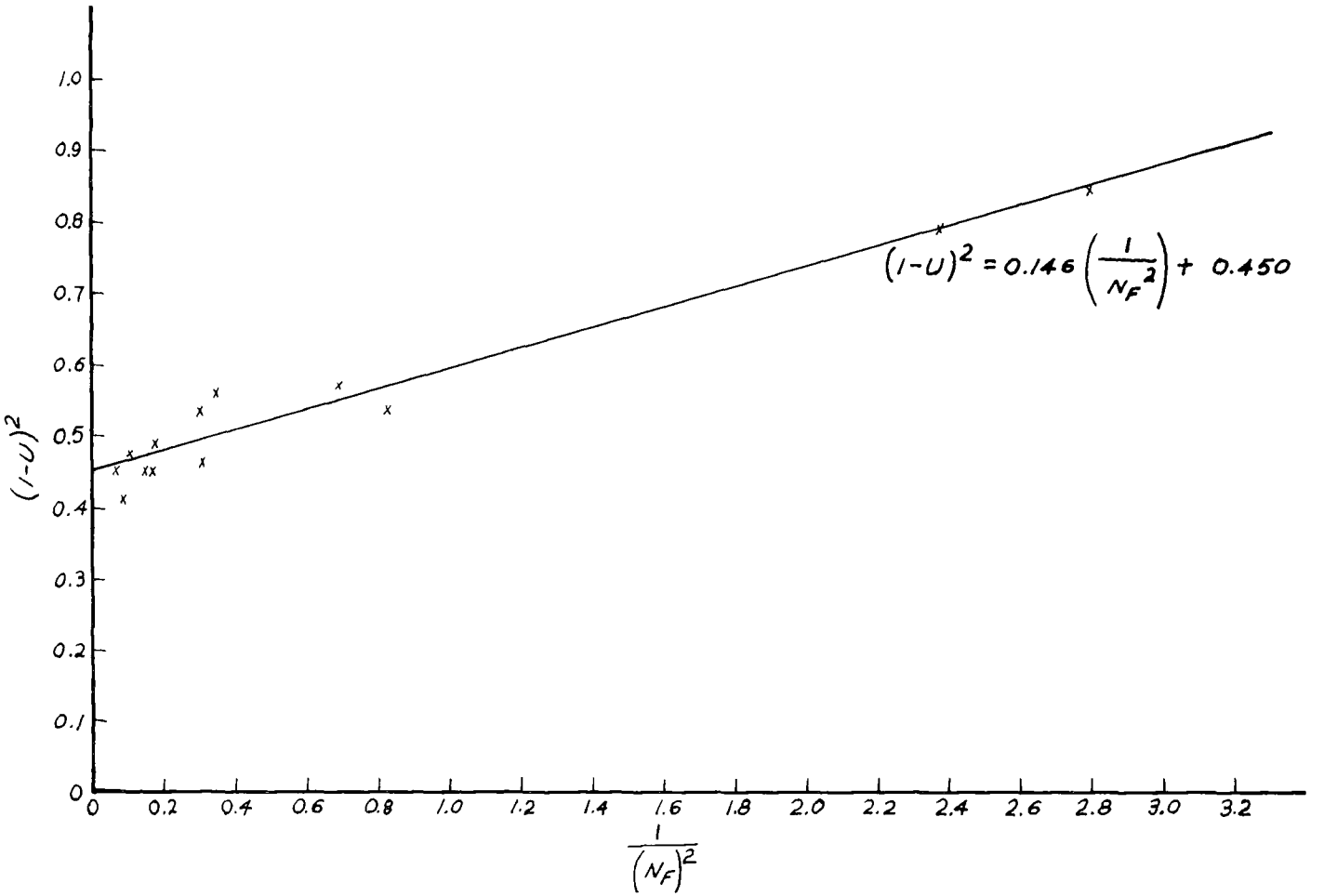

FIGURE 16. GENERALIZED SLICK TRANSPORT RELATIONSHIP BASED ON No. 2 FUEL OIL TESTS WHERE THE SLICK IS ORIENTED PARALLEL TO THE FLOW.

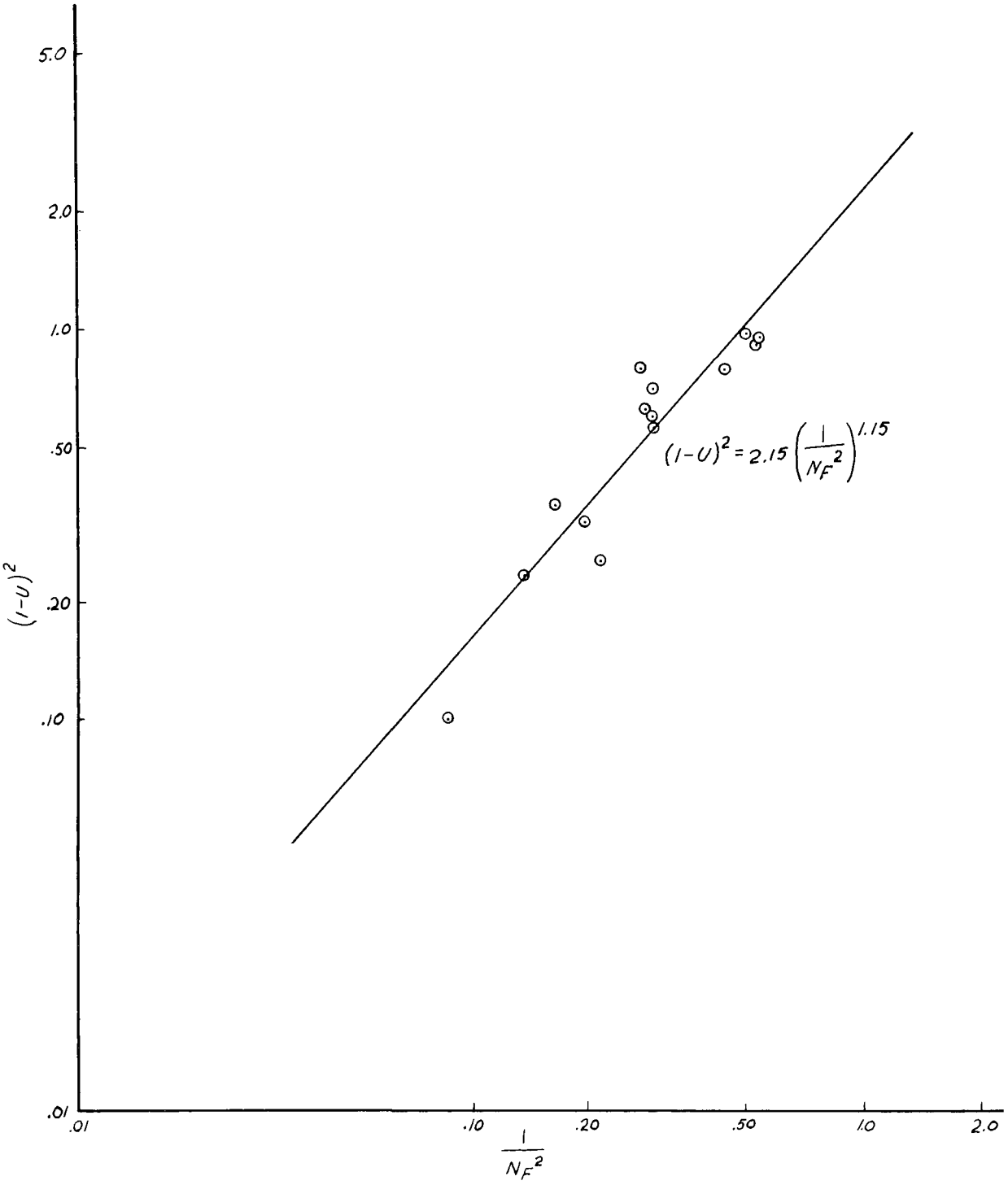

FIGURE 17. GENERALIZED SLICK TRANSPORT RELATIONSHIP BASED ON CRUDE OIL TESTS WHERE THE SLICK IS ORIENTED TRANSVERSE TO THE FLOW.

The exponent on the term $(1/N_F^2)$ is close to unity, indicating the approximate validity of the force balance. This relationship compares favorably with the linear relation found for larger values of U_w as plotted in Figure 15, but again, the use of the linear relationship is not reasonable when trying to predict threshold velocity. Also recognize that B_2 is not a pure constant, but rather contains the factor (ℓ/h). Generally, as the crude oil slick orients itself transversely to the flow, the ℓ dimension narrows to the point when it is comparable with h so that the ratio may approach a constant. However, this cannot always be assumed to be true and, as such the range of validity for this value of B_2 is limited.

APPLICATION OF RESULTS

Equations 78 and 79 or 80 may be used directly to calculate the speed of advance for No. 2 fuel oil slicks and crude oil slicks, respectively, under a smooth ice sheet. In order to apply the more generalized predictive relationship of Equations 85 and 89, the oil properties must be known. In addition, it is important to know whether a slick will tend to orient itself longitudinally with the flow, or tend to allign itself transverse to the flow. This behavior is probably viscosity dependent; however, tests with only two types of oil are insufficient for the establishment of a single relation which takes this factor into account. This complication does not necessarily detract from the ability of field personnel to use the generalized predictive relationship however, since in many river spills it will be relatively easy to observe the slick orientation through the ice cover. The selection of the proper predictive relationship is then based on the slick orientation, and with a knowledge of the oil properties and the current velocity, the slick velocity can be predicted as shown in the following sample calculations.

Slick Oriented Parallel to Flow

Consider a No. 2 fuel oil spill beneath smooth river ice. The density of the oil is 0.86 grams/cm^3. The interfacial surface tension for the No. 2 oil is typically 10 dynes/cm, and the contact angle is 135°. The mean current velocity is 20 cm/sec. Then from Equation 66, the equilibrium slick thickness can be calculated as follows:

$$h = \frac{2\sigma_o}{\Delta\rho_{iw} g}(1 - \cos\alpha) = \frac{(2)\ (10)\ (1.71)}{(0.14)\ (1)\ (980)} = 0.50 \text{ cm} .$$

Calculating the densimetric Froude number gives:

$$N_F{}^2 = \frac{U_w{}^2}{\Delta g h} = \frac{(20)^2}{(0.14)\ (980)\ (0.5)} = 5.83$$

Then, since No. 2 fuel oil will remain aligned with the mean flow, Equation 85 is used to determine the slick velocity as follows:

$$\left(1 - \frac{U_s}{U_w}\right)^2 = \frac{0.146}{N_F{}^2} + 0.450$$

or

$$\left(1 - \frac{U_s}{20}\right)^2 = \frac{0.145}{5.83} + 0.450 = 0.475$$

Solving for the slick speed, U_s, we find the oil slick velocity to be about 6.2 cm/sec.

Slick Oriented Transverse to the Flow

Consider a crude oil spill beneath smooth river ice. The density of the oil is 0.91 grams/cm^3. The interfacial surface tension for the crude oil is typically 38 dynes/cm and the contact angle is 160°. The mean current velocity is 20 cm/sec. Then from Equation 66, the equilibrium thickness is found to be:

$$h = \frac{2\sigma_0 (1 - \cos\alpha)}{\Delta\rho_w g} = \frac{2(38)(1.94)}{(0.089)(1)(980)} = 1.3 \text{ cm}$$

The densimetric Froude number becomes:

$$N_F = \frac{U_w^2}{\Delta g h} = \frac{(20)^2}{(0.089)(980)(1.3)} = 3.53$$

Crude oil slicks orient themselves transversely to the mean flow, therefore Equation 89 applies:

$$\left(1 - \frac{U_s}{U_w}\right)^2 = 2.15 \left(\frac{1}{N_F^2}\right)^{1.15}$$

or

$$\left(1 - \frac{U_s}{20}\right)^2 = 2.15 \left(\frac{1}{3.53}\right)^{1.15} = 0.50$$

Solving for the slick speed U_s, we find that the oil will move at about 5.8 cm/sec.

REFERENCES

1. Campbell, W.J., and S. Martin, "Oil and Ice in the Arctic Ocean: Possible Large-Scale Interactions," *Science*, July, 1973, pp. 56-58.

2. Barber, F.G., "Report of the Task Force-Operation Oil (Clean-up of the Arrow Oil Spill in Chedabucto Bay)," Ministry of Transport, Canada, 1971.

3. Glaeser, LTJG J.L., USCGR, LCDR G.P. Vance, USCG, "A Study of the Behavior of Oil Spills in the Arctic," *Final Report*, U.S. Coast Guard, Washington, D.C., February, 1971.

4. Golden, P.C., "Oil Removal Techniques in Our Arctic Environment," *Marine Technology Society Journal*, Vol. 8, No. 8, January,1974, pp. 38-43.

5. Fay, J.A., "In Oil on the Sea," ed. D.P. Hoult, 5-13, New York: Plenum, 1969.

6. McMinn, T.J., "Oil Spill Behavior in a Winter Arctic Environment," Offshore Technology Conference, Paper Number OTC 1747, 1973.

7. Chen, E.C., J.C.K. Overall, and C.R. Phillips, "Spreading of Crude Oil on an Ice Surface," *Canadian Journal of Chemical Engineering*, Vol. 52, February, 1974.

8. Hoult, D.P., "Oil Spreading on the Sea," *Annual Review of Fluid Mechanics*, Vol. 4, 1972, pp. 341-368.

9. Hoult, D.P., "Oil in the Arctic," *Report No. CG-D-96-75*, USCG, Office of Research and Development, Washington, D.C., February, 1974.

10. Mackay, D., M. Medir, D. Thornton, "Interfacial Behavior of Oil Under Ice," *Canadian Chemical Engineer*, Vol. 54, February/April, 1976.

11. Jeffreys, "On the Formation of Water Waves by Wind," *Royal Society Proceedings A*, Vol. 107, 1925.

12. Jirka, G., G. Abraham, D. Harleman, "An Assessment of Techniques for Hydrothermal Prediction," Ralph M. Parsons Laboratory for Water Resources and Hydrodynamics, *Report No. 203*, July, 1975.

TECHNICAL REPORT DATA
(Please read Instructions on the reverse before completing)

1. REPORT NO.	2.	3. RECIPIENT'S ACCESSION NO.
EPA-600/3-79-041		

4. TITLE AND SUBTITLE	5. REPORT DATE
Transport of Oil Under Smooth Ice	April 1979 issuing date
	6. PERFORMING ORGANIZATION CODE
	220C

7. AUTHOR(S)	8. PERFORMING ORGANIZATION REPORT NO.
M.S. Uzuner, F.B. Weiskopf, J.C. Cox, L.A. Schultz	

9. PERFORMING ORGANIZATION NAME AND ADDRESS	10. PROGRAM ELEMENT NO.
ARCTEC, Incorporated 9104 Red Branch Road Columbia, Maryland 21045	11. CONTRACT/GRANT NO. 68-03-2232

12. SPONSORING AGENCY NAME AND ADDRESS	13. TYPE OF REPORT AND PERIOD COVERED
Environmental Research Laboratory--Corvallis Office of Research and Development U.S. Environmental Protection Agency Corvallis, Oregon 97330	Final 14. SPONSORING AGENCY CODE EPA/600/02

15. SUPPLEMENTARY NOTES

Contact: Barry Reid, Corvallis, OR 97330 503/757-4607 (FTS 420-4607)

16. ABSTRACT

Previous studies of oil-ice interaction have been limited to spreading under quiescent conditions. The present study examines the current driven spread of oil under a smooth ice cover. Generalized relations between current speed and oil transport rate are developed and found to be strongly dependent upon the orientation of the oil slick to the direction of current flow. Methods for application are presented.

17. KEY WORDS AND DOCUMENT ANALYSIS

a. DESCRIPTORS	b. IDENTIFIERS/OPEN ENDED TERMS	c. COSATI Field/Group
Oil spill Arctic pollution Oil-ice-current interaction	Crude oil No. 2 fuel oil	

18. DISTRIBUTION STATEMENT	19. SECURITY CLASS *(This Report)*	21. NO. OF PAGES
Release to public	Unclassified	
	20. SECURITY CLASS *(This page)*	22. PRICE
	Unclassified	

EPA Form 2220-1 (Rev. 4-77)

☆ U.S. Government Printing Office: 1979—698-323/140